This is to certify that the

thesis entitled

Bench Scale Studies of HF Saccharification of Wood
With a 1.5 Liter Packed Bed Reactor

presented by

Mark Lealand Reath

has been accepted towards fulfillment
of the requirements for
M. S. degree in Chemical Engineering

Major professor

Date June 4, 1989.

BENCH SCALE STUDIES OF HF SACCHARIFICATION OF WOOD WITH A 1.5 LITER PACKED BED REACTOR

By

Mark Lealand Reath

A Thesis

Submitted to
Michigan State University
in partial fulfillment of the requirements
for the degree of

Master of Science

Department of Chemical Engineering

1989

ABSTRACT

BENCH SCALE STUDIES OF HF SACCHARIFICATION OF WOOD WITH A 1.5 LITER PACKED BED REACTOR

By

Mark Lealand Reath

A bench scale facility to react gaseous hydrogen fluoride (HF) with wood was characterized with 100 g beds of (16 mm x 29 mm x 5mm) wood chips, at temperatures of 45, 55, and 63 °C; nominal HF flow rates of 0.75, 1.4, and 5.8 g/min; and N_2 flow rates of 0.75, 4.0, and 6.0 slpm. Loading data were gathered during adsorption and desorption; these data are specific to the particular reaction configuration. Approximately 120-180 minutes were required to adsorb HF to within 90-100% of equilibrium. At the conditions studied, desorption required 35-40 hours to reach a level of 5-15% HF. The adsorption and desorption had negligible dependence on flow rate in the range of conditions studied. About 3-5% volatile reaction products were formed. The reacted substrate was 35% soluble in water at 50 or 100 °C, and 65% soluble in 3% H_2SO_4 at 121 °C.

This work is dedicated to my dear wife, Lisa, for her continued love, understanding and encouragement.

ACKNOWLEDGMENTS

The author wishes to thank Dr. Martin Hawley, Dr. Derek Lamport and Gregory Rorrer, for their helpful comments and advice, and also the State of Michigan Research Excellence Fund for financial support.

TABLE OF CONTENTS

LIST OF TABLES

LIST OF FIGURES

KEY TO ABBREVIATIONS

Abbreviation	Description
$^{\circ}C$	Degrees Celsius
cm	Centimeters
g	Grams
hr	Hours
Kg	Kilograms
kPa	Kilopascals (Pressure, note that all pressures cited are at gauge pressure.)
min	Minutes
ml	Mililiters
mm	Milimeters
wt.%	Weight Percent
sch-80	Schedule 80 pipe specification
slpm	Standard Liters per Minute (Gas volumetric flow rate at standard temperature and pressure.)

INTRODUCTION

A. The Need for Biomass Conversion

The concept of obtaining liquid fuel and chemicals from biomass has been around for many years. Existing processes, suffering from high costs and low yield, have been unable to compete economically with petroleum based processes (Hawley, Selke, & Lamport, 1983). However, depletion of this resource, combined with the instability of many of its major sources, renders it prudent to explore and optimize biomass conversion processes. Hydrogen fluoride, (HF), saccharification has shown the potential to be an economical step in the conversion of biomass to useful products. It is through this and similar processes that a renewable, self-supporting source for chemical raw materials can be developed.

B. Characteristics of Lignocellulosic Materials

"Lignocellulose", is the term given to a wide class of biomass that form the structural components (trunks, stems, branches, etc.) of plants. Useful sources of lignocellulosics include wood, wood waste, and agricultural residues. Lignocellulosic materials contain primarily three classes of components; cellulose, hemicellulose, lignin, and a minor amount of extractives, and acetyl compounds. These terms refer to general groups of compounds with similar properties, reflecting the complexity and variability of lignocellulosic composition. It should be noted that analytical methods used to selectively isolate these groups are approximate; a method that affects one group almost invariably affects the other. In spite of this, group analysis methods have proven invaluable for industrial applications (Wenzl, 1970).

Cellulose, a glucose polymer, forms a crystalline network through β (1-4) glycosidic linkages and extensive hydrogen bonding. The cellulose fibers link to form bundles, and give rigidity and structure to lignocellulosic materials. Hemicellulose is a semi-amorphous polymer of five and six carbon sugars. Hemicellulose constituents include: xylose, mannose, galactose, arabinose, and uronic acid. Lignin is a complex, three dimensional amorphous polymer composed primarily of phenylpropane units. The relative amounts of these groups as well as their individual compositions vary widely with: plant species, growth location, climate, age, and physiological function of the sample. For example, deciduous woods contain approximately: 45-47% glucan, 16-25% xylan, 15-25% lignin, 3-5% uronic acid, 2-3% mannan, 1% galactan, .5% araban (Timell, 1957).

Bigtooth Aspen (Populus Grandidentata) wood was selected for saccharification study at Michigan State University. This species is representative of those most likely to be used in the "energy plantations" of the future, due to its growth and propagation characteristics. This variety is very similar to Trembling Aspen, (Populus Tremuloides) (Rorrer, 1989) with the following composition: 55.2% glucan, 15.4% xylan, 15.7% lignin, 3.2% uronic acid, 2.2% mannan, .8% galactan, .4% araban, 3.6% extractives, and .2% ash (Timell, 1957).

C. Processing of Lignocellulosic Materials

In any process utilizing lignocellulosic materials, it is advantageous to preserve the existing chemical reactivity of the substrate. In this way, the chemical functionality of the resulting products is maximized, permitting diversified product utilization. When used as fuels, lignocellulosics are greatly underutilized, from a chemical standpoint, because the major products are H_2O and CO_2. In paper production, the lignin and hemicellulose are reacted and dissolved, preserving the cellulose, but taking little advantage of the hemicellulose and lignin components. Saccharification processes are the least destructive, and permit the utilization of all three classes of components to give cellulose, hemicellulose, and lignin derivatives.

Saccharification involves the depolymerization of cellulose and hemicellulose to yield monomeric and oligomeric sugars. The sugars can be used for fermentation and catalytic conversion processes. The residual lignin can be used to produce organic feedstocks. Hence, saccharification may serve as an optimal unit operation in the biomass conversion process.

D. The Saccharification Reaction

The saccharification (hydrolysis) of lignocellulosics can be accomplished using enzymes, or strong acids in dilute or concentrated form. Major drawbacks of some processes include low yield, long reaction times, high reactant cost, uneconomical reactant recovery, and sugar degradation. Preliminary results suggest that hydrogen fluoride, (HF), saccharification minimizes these drawbacks (Hawley, Selke, & Lamport, 1983).

HF saccharification is fundamentally different from other acid and enzymatic hydrolyses in mechanism. Rather than hydrolysis proceeding via protonation of a hemiacetal oxygen, HF saccharification involves the formation of glycosyl fluoride followed by solvolysis of the fluoride, regenerating HF:

$$(\text{sugar})n \xrightarrow{(\text{HF})} n(\text{sugar.F}) \xrightarrow{(\text{H}_2\text{O})} n(\text{sugar}) + \text{HF}$$

$$[\text{cellulose}] \longrightarrow [\text{sugar fluorides}] \longrightarrow [\text{sugar oligomers}] + \text{HF}$$

Anhydrous HF, in either gas or liquid form, quickly reacts with wood at ambient conditions to give high yields of sugar fluorides. The sugar fluorides are readily hydrolyzed to sugar oligomers in the presence of water.* The acid can be removed (desorbed) from the substrate using a carrier gas at temperatures up to 100 °C to yield a solid mixture of monomeric sugars, oligomeric sugars, and lignin. The room temperature boiling point of HF (19.5 °C) makes both gas-phase and liquid-phase reactions feasible at atmospheric pressure, with HF recovery and recycle. An important feature of HF saccharification is near quantitative yields of both cellulosic and hemicellulosic sugars in a single adsorption/reaction step while reducing the formation of sugar degradation products.

Three basic processing stages are required for HF saccharification: HF adsorption, HF reaction (dwell time), and HF desorption. These stages are illustrated in Figure 1. During the adsorption stage, the HF vapor is loaded onto the the substrate at temperatures of 30-65 °C. The HF reaction stage may be required to provide enough time for the HF to

---

*In a commercial process, the water required for hydrolysis would be available in the air dried substrate, (5-15% moisture).

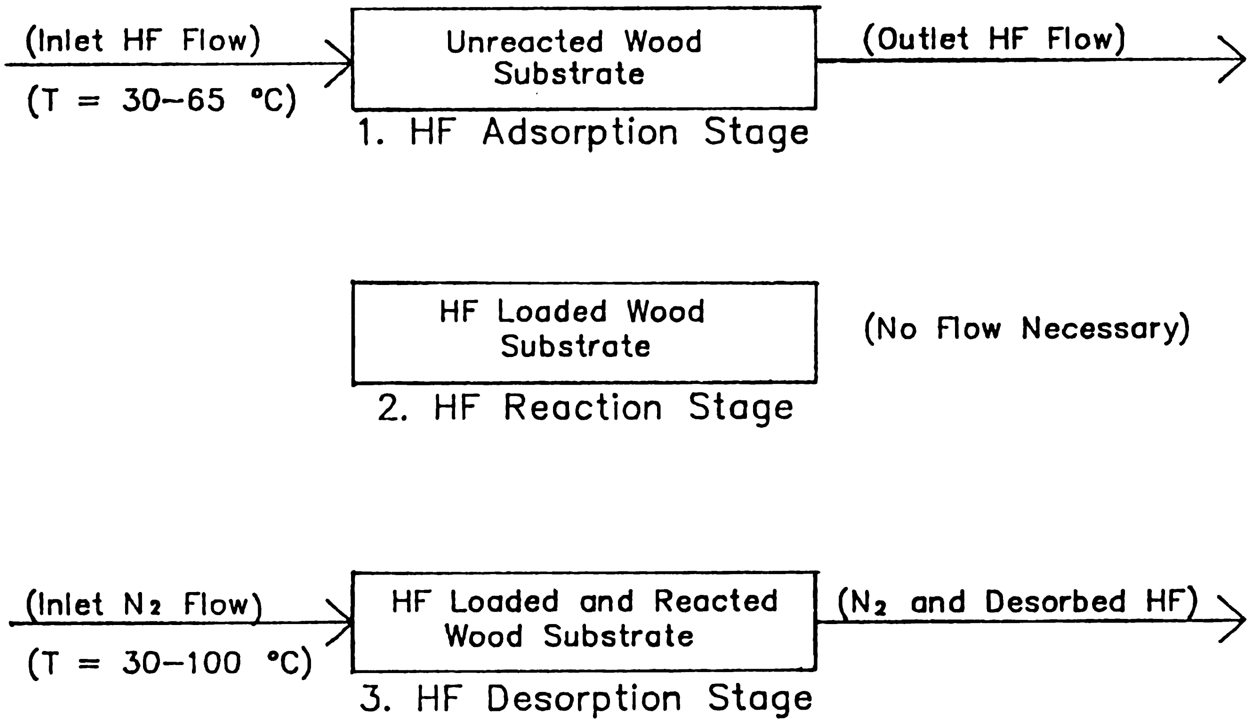

Figure 1, Stages Required for HF Saccharification completely depolymerize the cellulose and hemicellulose components. During the desorption stage, the HF is removed from the substrate by an inert carrier gas at temperatures between 30 and 100 °C.

Conceptually, HF saccharification has the following potential advantages over other methods of acid hydrolysis (Hawley, Selke, & Lamport, 1983):

1. Near ambient reaction conditions.
2. Short reaction times.
3. Ability to utilize standard-size substrate chips.
4. Minimization of degradation reactions.
5. Feasible acid recovery.
6. Production of useful lignin by-product.

These advantages lead researchers to study the characteristics of HF saccharification. The next section summarizes the results of these investigations.

E. Literature Review of HF Saccharification

The ability of HF to break down cellulose into sugars has been known since 1869 (Gore, 1869). The commercial availability of anhydrous HF renewed interest in this reaction in the late 1920's. This research was aimed at the development of alternative fermentation sugar sources.

In 1933, German researchers published the results of their recent work with HF hydrolysis of cellulose and sprucewood (Fredenhagen & Cadenbach, 1933). In these experiments, HF vapor was condensed onto 100 grams of ground wood, previously cooled to 0 °C. A 1:1 HF to wood ratio was required for high polysaccharide conversion. Vacuum evaporation was required to reduce the residual HF level below 1%. It was found that the substrate moisture content affected the product solubility by controlling the degree of polymerization of the reversion products.

Unfortunately, only the results were published, a detailed account of the data were not.

A pilot plant based on HF vapor hydrolysis was constructed and operated in Germany in the mid-1930's (Luers, 1938). The design included agitated, jacketed reactors, capable of cooling and heating the substrate. The reactors operated under partial vacuum during the HF adsorption, dwell time, and desorption cycles, to ensure proper HF distribution and to facilitate intraparticle HF transport. A 40% HF loading was found to give optimum carbohydrate conversion. A dilute acid post hydrolysis followed the HF treatment, to ensure complete extraction of the reaction products. An HF/acetic acid separation was incorporated to separate HF from the acetic acid by-product before HF recycle.

Research into HF saccharification ceased in the late 1930's with the advent of World War II. However, the oil crisis of the 1970's renewed western interest in this area. In 1979, research efforts began in the United States, France and Denmark. These have been joined by efforts in West Germany and Canada.

Researchers in France (Defaye, Gadelle, Padopoulos, & Pedersen, 1983; Defaye, Gadelle & Pedersen, 1981) have investigated the nature of the lignin by-product, and have studied the bonding in oligomeric reaction products. It was found that the lignin ether and ester linkages are not cleaved by HF, but temperature- and time-dependent autocondensation may occur. It was determined that long HF exposure will cause lignin degradation. These studies indicated that the processing of oligomeric reaction products will be important to future applications of HF saccharification.

West German researchers (Franz, Erckel, Riehm, Wonernle, & Deger, 1982; Franz, Fritsche-Lang, Deger, Erckel, & Schlingmann, 1985) have used a small (10 g) bench scale system to study HF adsorption and desorption onto sprucewood. A Claussius-Claperyon approach was used to calculate the desorption enthalpy. The desirability of a prehydrolysis stage was investigated. The oligomeric liquid phase reaction products were also characterized.

In Denmark, (Bentsen, 1982; Reffstrup & Kau, 1985; Reffstrup, 1986) the HF vapor saccharification of barley straw has been investigated with a variety of reaction configurations. The formation new chemical linkages between sugars and lignin apparently occurred with prolonged HF exposure. A small, (< 7 kg/hr) pilot plant with a twin screw extruder reactor was developed and characterized. The viscosity of the resulting HF/straw mixture was measured with this apparatus. Feasible HF desorption, high carbohydrate yield, and reaction product fermentation were demonstrated.

The largest modern saccharification pilot plant was developed in Canada (Ostrovski, Aitken, Free, & Duckworth, 1984; Ostrovski, Aitken, & Hayes, 1985). The reactor was capable of processing 20 kg of aspen chips per batch, while obtaining gas and substrate samples. The reactor apparently contained some form of mild agitation, but the exact configuration is undisclosed. The global processing characteristics were investigated, including substrate moisture content, processing time, and processing temperatures. These results are not published due to patent restraints.

Early research at Michigan State University verified high sugar yields obtained in the liquid phase reactions, demonstrated the existence of the glycosyl fluoride intermediates, and showed that the residual fluoride content of the reaction products can be made very low (under 0.4%) (Hardt & Lamport, 1982; Lamport et al., 1981; Selke, et al., 1982).

More recently, MSU researchers have investigated the gas phase reaction; this process is believed to have the greatest commercial potential due to its low acid throughput. The reaction rates of gas phase HF hydrolysis have been investigated with (20 mg) microscale reaction systems. (Rorrer, Ashour, & Hawley, 1987; Rorrer, Hawley & Lamport, 1986; Rorrer, Mohring, Hawley, & Lamport, 1988; Rorrer, Mohring, Lamport, & Hawley, 1988). Intrinsic reaction rates were measured in the absence of external mass transfer resistances. A nonisothermal reaction model was developed to predict the behavior of a single particle during HF adsorption. High yields of sugars were obtained with the microscale system. Other issues including: oligomer distribution, substrate moisture content, and lignin-glucose condensation were also addressed.

The HF adsorption/desorption isotherms were obtained at MSU with a gravimetric microscale apparatus (Rorrer, Mohring, Hawley & Lamport, 1988; Mohring & Hawley, 1989). A Classius-Claperyon analysis was used to calculate the heat of HF desorption over a 30-80 °C temperature range. A macroscopic (85 mg) particle experiment was also performed to investigate the heat transfer effects in a larger wood chip. The results indicated that the adsorption results were influenced by heat transfer resistances.

F. Justification for Research at the Bench Scale

Previous experiments did not provide the necessary data to predict the behavior of a commercially applicable reaction system. To develop the design for such a system, basic engineering data are needed. This has lead to the development of larger, bench scale experiments to study these effects. The bench scale reaction facility will enable researchers to study the following characteristics important to the commercial application of HF saccharification:

1. The utilization of different lignocellulosic substrates.
2. The formation of saccharification by-products.
3. The feasibility and requirements of HF recovery.
4. The optimal conditions for HF adsorption/desorption.
5. Characterization of sugars and lignin.
6. Production of sugars and lignin for utilization studies.

G. Experimental Objectives

The following are specific goals of this study:

1. Design and construct a gravimetric apparatus to measure the HF uptake of a packed bed of standard-sized wood chips, capable of processing up to 250 grams of wood per batch.

2. Obtain HF loading versus time data for different temperatures and flow rates during adsorption and desorption.

3. Obtain reacted wood samples for visual inspection, solubility measurements, and sugar yield analysis.

The HF uptake (HF loading) is a measure of HF concentration in the substrate, and is expressed as a percentage of the wood weight. The gas phase HF saccharification reaction forms non-volatile reaction products. Therefore, the weight change of the substrate is a good measure of the HF loading. The bench scale apparatus obtained this measurement by a continuous monitor of the weight of a packed bed reactor during the adsorption/desorption cycles.

The initial characterization experiments evaluated the dependence of the adsorption and desorption profiles on temperature and flow rate. The reaction product was also evaluated, extracted, and stored for later sugar distribution analysis.

The reaction configuration presented here was intended to be the first generation of bench scale reactors at MSU. Knowledge gained from these initial experiments will allow improvements to be incorporated into subsequent reactor configurations.

EXPERIMENTAL

A. Apparatus Description

1. Summary of Facility Design Specifications

The knowledge gained from previous experiments helped to specify the characteristics of the bench scale system, which are summarized in Table 1. The reactor had the capability of processing up to 250 grams of wood chips in a packed bed configuration.

Table 1, Specifications of the Bench Scale System

1.	Maximum reactor capacity	250 grams
2.	Temperature range	40-70 °C
3.	HF flow rate	0-10 g/min
4.	HF backpressure	15-30 kPa (upstream of flowmeter)
5.	Reactor pressure	atmospheric
6.	Heat tracing temperature	45-60 °C
7.	Materials of construction:	
	a. Valves	Monel/Kel-F/Viton
	b. Tubing	Monel
	c. Fittings	Monel, Steel, 316 Stainless Steel
	d. Reactor vessel	Copper, Brass
	e. Parts exposed to moisture	Teflon, PVC, Polyethylene

The bench scale apparatus operated on the same principle as the MSU microreactor systems; the HF was adsorbed at a lower temperature and desorbed into flowing nitrogen. The only variation was in the reactor configuration. Instead of using a single 20 mg chip, the bench scale studies utilized a 100 g packed bed of standard-sized (16 mm x 29 mm x 5 mm, (± 2 mm)) chips.

Figure 2 is a general illustration of the bench-scale apparatus. The design was divided into three basic systems; HF supply system,

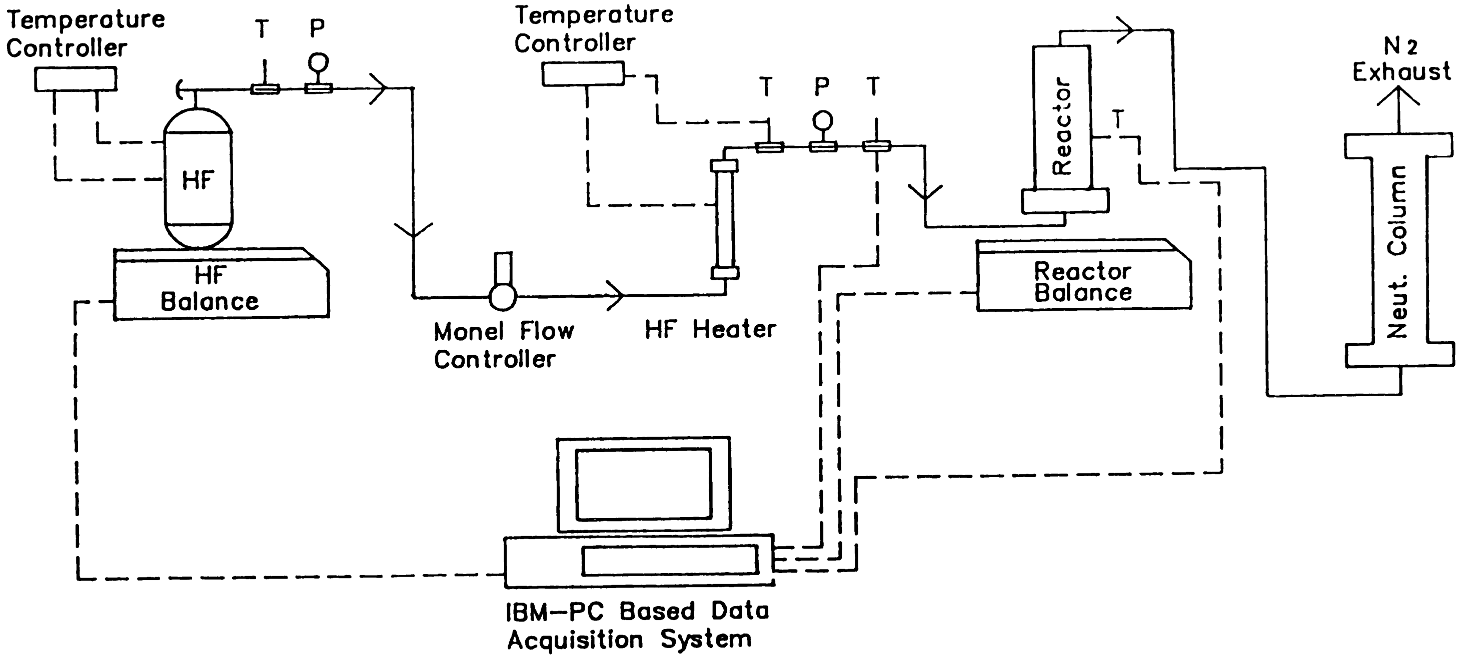

Figure 2 The Bench Scale Saccharification Facility

reaction system, and neutralization system. In the HF supply system, the acid was evaporated from a standard cylinder and metered at a constant flow rate through an electronic mass flow controller. In the reaction section the HF contacted the packed bed of wood chips. The rates of adsorption and desorption were monitored gravimetrically. The excess and desorbed HF was safely neutralized in a packed countercurrent absorption column.

All lines in contact with HF were composed of 6.4 mm or 9.5 mm Monel tubing, and were heated with standard laboratory heating cord. The heat tracing was required to ensure that HF did not condense at any point in the system. The HF vapor flow rate was regulated by a Matheson model 8203 Monel mass flow controller, with a nominal range of 0-10 g/min HF. All valves were of Monel/Kel-F construction, chosen to minimize the pressure drop through the system.

Gravimetric measurements were obtained for the HF tank and reactor. This permitted a monitor of the HF adsorption/desorption in the reactor, and a continuous on-line calibration of the mass flow controller. (The flow controller calibration was required because of the wide variation of HF physical properties in the range of operating conditions.) The gravimetric measurements were made with Sartorius model 3808-MP8 top loading balances with a range of 0-30 Kg, (± 0.1g) controlled via RS-232 serial interface to an IBM-PC/XT.

The gas temperature entering the reactor was measured and controlled with an inconel-sheathed type-T thermocouple. The reactor and HF tank surface temperatures were measured with type-T surface thermocouples. The thermocouple signals were interfaced to PID temperature controllers connected to the inlet gas heater, the HF tank heater, and the reactor heater. The gas inlet temperature and reactor temperature were interfaced to an IBM PC/XT-based data acquisition system.

The excess and desorbed HF was neutralized in a column fabricated from 15 cm sch-80 PVC piping, 91 cm long, filled with 12 mm polyethylene rashig rings. A caustic neutralization solution was continuously circulated through the column.

2. The HF Supply System (Figure 3)

The HF supply system originated with a standard 1.5 Kg HF cylinder. The cylinder was electrically heated to maintain a constant flow of vapor. The vapor leaving the cylinder was passed through a manual control valve to regulate the pressure upstream of the flow controller to a level of 15-30 kPa. The vapor passed through a manual purge valve that permitted the HF supply system to be purged with nitrogen. The entire cylinder/purge valve assembly was mounted on the top loading balance, and was connected to the remaining apparatus with Teflon-lined flexible tubing. The HF vapor then passed through a remote control purge valve, so that the entire system could be purged from a remote location, as a safety measure. The pressure of the vapor was measured by a Monel pressure gauge, to determine the conditions measured by the mass flow controller. (During system operation, the pressure was maintained near 17 kPa, ± 3.5 kPa to assure a constant HF flow rate.) The HF vapor left the supply system at a constant flow rate near atmospheric pressure.

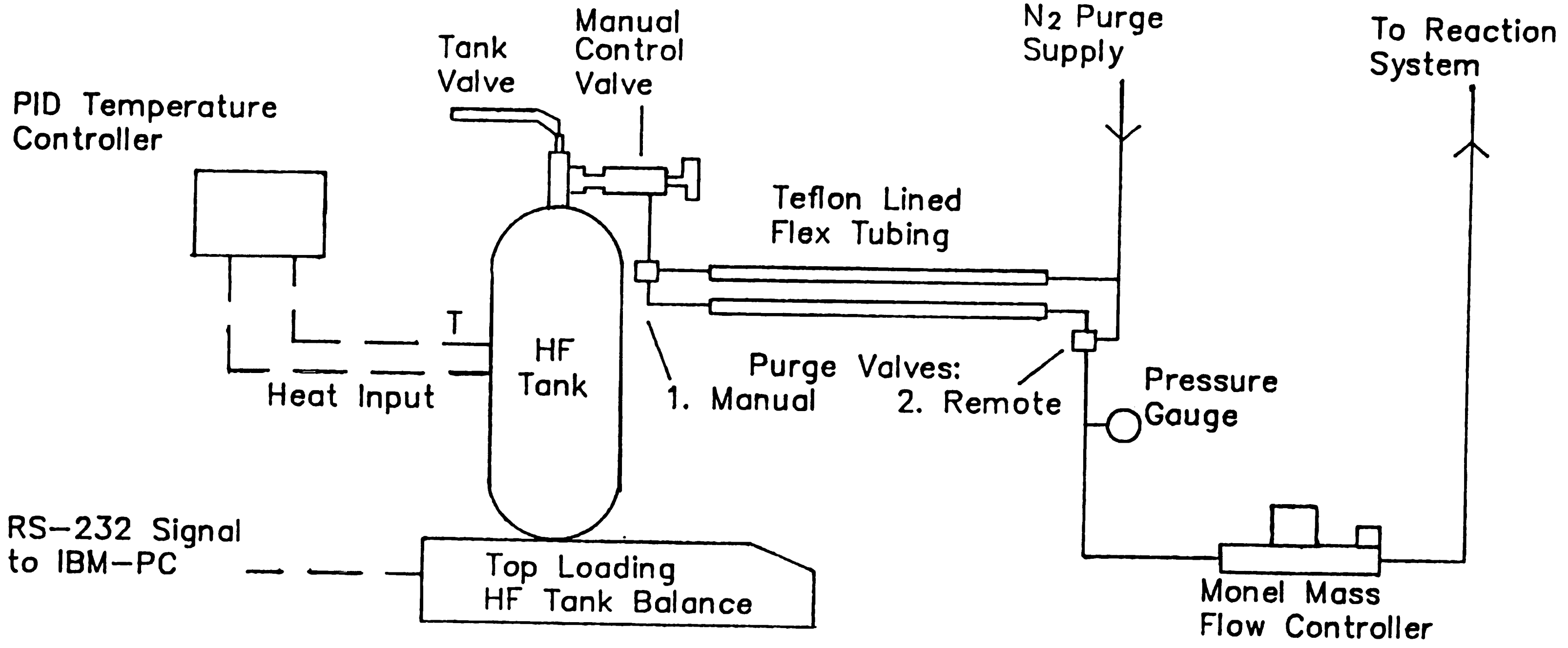

Figure 3 The HF Supply System

3. The Reaction System (Figure 4)

The vapor from the HF supply system flowed to the reaction system. Here, the temperature of the entering gas was controlled by a feedback PID controller to within ± 1.0 C. The gas passed through a remote control bypass valve that permitted the flow to be diverted directly to the neutralization system. This allowed the reaction to be started after the initial transient fluctuations in temperature and flow rate. Once the valve was activated, the vapor flowed through Teflon-lined flexible tubes to the packed bed reactor.

The reactor was constructed of 7.6 cm copper tube with silver-soldered brass and copper fittings. Entrance to the reactor was achieved through a 7.6 cm PVC flange assembly. The reactor surface temperature was controlled with a PID temperature controller. This surface temperature was interfaced to the microcomputer and served as an estimate of the vapor temperature during the reaction. The reactor was covered with 3.2 mm of fiberglass insulation to prevent excessive heat loss, and to ensure even heating. The entire reactor assembly was mounted vertically to minimize vapor channelling around the bed.

Within the reactor, the wood chips were held by a polyethylene mesh basket, designed to ensure a tight fit to the reactor wall. In addition to facilitating sample removal, the design of the basket created a 500 ml dead space at the bottom of the reactor. This allowed the entering vapor to equilibriate with the wall temperature during its 20 second residence time in this section. The reactor served as a thermal ballast against temperature fluctuations of the inlet vapor.

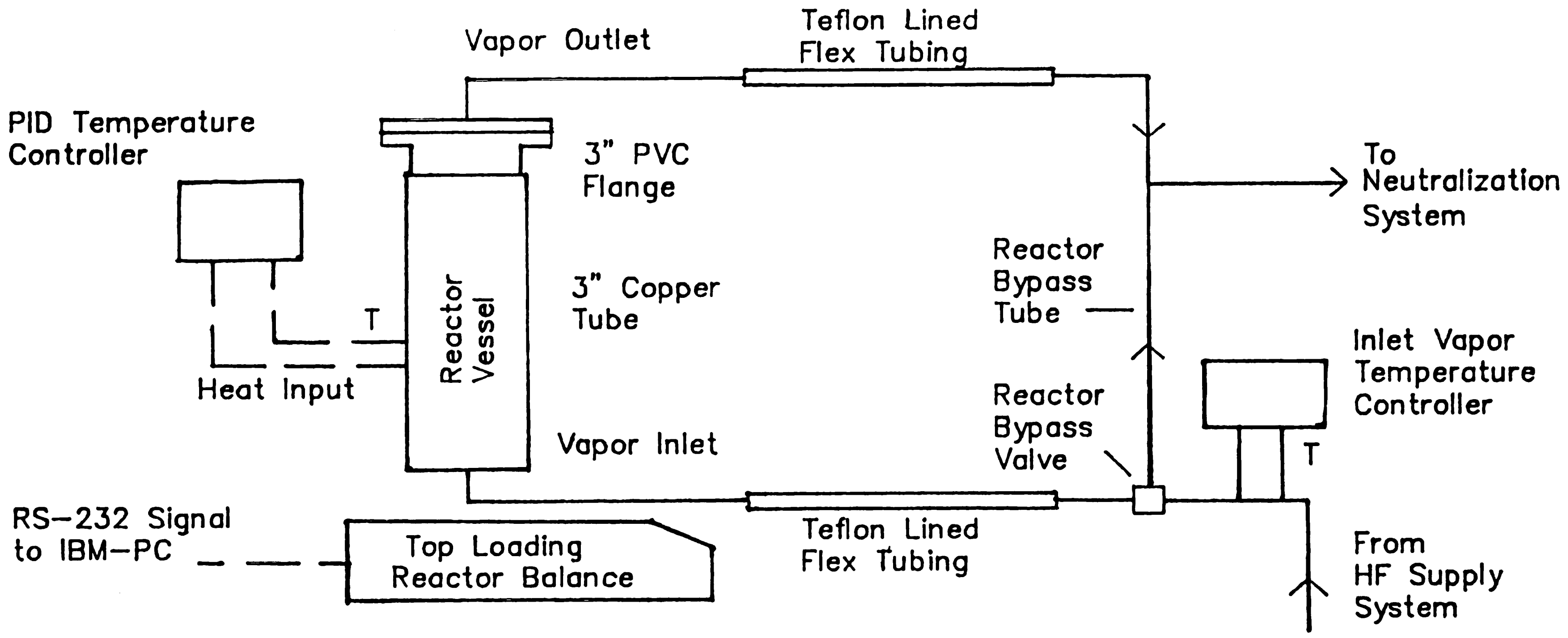

Figure 4 The Reaction System

4. The Neutralization System (Figure 5)

Once the vapor exited the reactor, it flowed to the neutralization system. To guard against corrosion, the tubing was changed from 9.5 mm Monel to 9.5 mm Teflon prior to entry to the neutralization column. The acid was continuously neutralized with an aqueous solution of potassium hydroxide, circulated at 10 liters/min, and stored in 114 and 208 liter polyethylene tanks. The maximum temperature rise was kept below 5 °C with this configuration. The pH of the circulating solution was continuously monitored to determine when the caustic solution needed recharging.

An additional benefit from this configuration was that the total amount of HF used in the system could be estimated by recording the amount of KOH added to the neutralization solution. This record was used to determine when HF tank replacement was necessary.

5. Safety Considerations

HF vapor is highly toxic in any form of exposure. Initially, HF causes skin burns similar to those caused by other acids. However, HF burns differ from other acid burns in that the fluoride ion readily penetrates the skin and destroys the underlying tissue layers. The symptoms of HF exposure to the skin include severe burning pain, accompanied by a white discoloration of the skin. These symptoms occur immediately with exposure to acid concentrations above 50%, within 8 hours with concentrations of 20-50%, and within 24 hours with acid concentrations below 20%. Exposure to HF vapor also causes delayed effects.

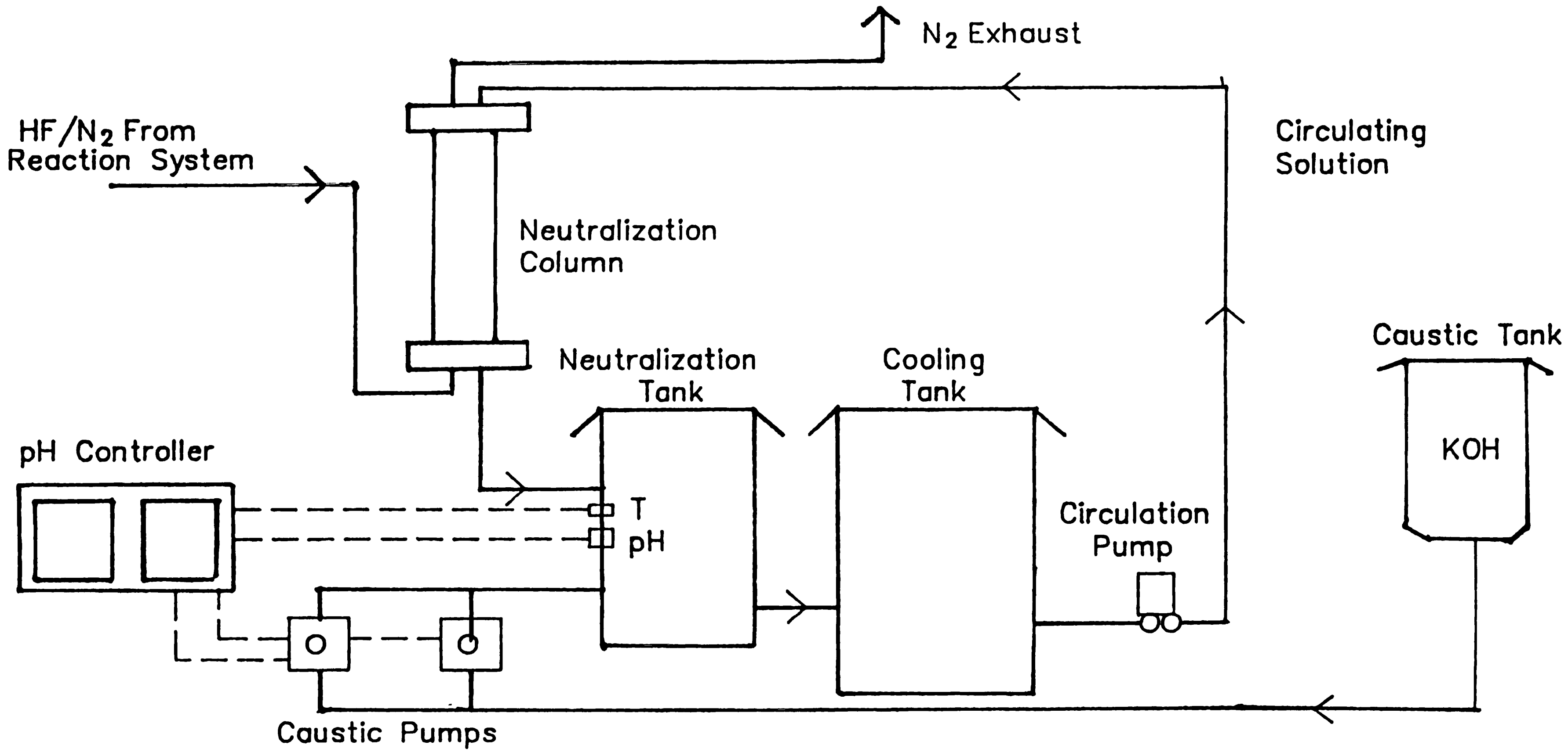

Figure 5 The Neutralization System

Medical and safety literature was obtained from an HF manufacturer, listing treatments required for various types of exposure. Aqueous solutions of Hyamine and Zephiran Chloride were recommended for topical treatment. Zephiran Chloride solutions (1:750 dilution) were prepared and stored in laboratory and home locations to be used in the event that exposure symptoms appear. A local hospital was informed of our activities, and was prepared to treat patients with HF exposure.

For safety considerations, the entire apparatus was constructed in a (7′ x 3′ x 16′) standing fume hood. Conventional safety equipment, (Viton gloves, lab coat, face shield), were worn during the operation of the experiment. In addition, a canister gas mask was used for all operations requiring entry into the hood.

The reaction system was designed for safe operation. The remote control valves permitted the entire apparatus to be purged without opening the hood. All electrical and pneumatic control connections originated outside the hood. This permitted the entire experiment to be shut down from a remote location.

The neutralization system was designed to be a key component in the safety program. The column size, (183 cm long, 15.2 cm diameter), liquid capacity, (320 l), and liquid circulation rate (10 liters/min), were greatly oversized. In the event of complete failure of the HF tank valve, a full tank of HF would produce only a 0.32% aqueous HF solution. In this unlikely event, the released HF vapor is safely contained for subsequent neutralization.

Certain safety procedures were always observed when handling HF, or HF contaminated objects. These precautions are summarized in Table 2.

Table 2, HF Facility Safety Precautions

1. Study literature regarding HF exposure. Know the symptoms of exposure and learn first aid procedures. Have necessary treatment solutions prepared and readily accessible.

2. Always wear Viton or Neoprene gloves when performing maintenance or repair work on the apparatus. Wear long sleeve clothing underneath lab coat and tuck sleeves into glove gauntlet.

3. Do not contaminate clothing by accidental glove contact.

4. Wash gloves with soap and water and dry with paper towel before removing gloves. Keep separate bar of soap for washing gloves.

5. Thoroughly wash hands after removing gloves.

6. Routinely swab hood sash and table surfaces with soap and water to remove fluoride residues.

7. Wash areas of suspected HF contamination with sodium bicarbonate solution. Watch for CO_2 bubble formation.

8. Treat all objects in the hood as if they are contaminated. Wash all tools in soapy water after use.

9. Remove HF tank safety cap after all other tank preparations have been performed. Wear face shield and Viton gloves during this operation. This must be done in the hood, as some HF may flash out of the valve. Connect the tank to the system as soon as possible.

10. Pressure test the tank connection with 70 kPa nitrogen before loosening the tank valve. Use leak detector to locate leak sources if necessary.

11. Tank valve is closed very tight at the factory. Never use hammer mallet to open tank valve. Instead, use pipe extension with tank valve wrench. Use a large crescent wrench on the valve body to counter the torque applied with the tank valve wrench. Wear face shield and viton gloves during this operation. Use same procedure to seal empty tanks before removal.

12. Pressure test the entire system with 70 kPa nitrogen before every run. Use leak detector if necessary.

13. Treat all reacted material as contaminated. Handle material with Viton gloves in fume hood.

B. Experimental Procedure

1. Operation of the Bench Scale Apparatus

Appendix B details the steps used in the operation of the bench scale experiment. A summary of these steps follows.

a. Sample Preparation and Reactor Loading

The purpose of the sample preparation and reactor loading operations was to charge the reactor with a characterized chip loading and to prepare the reactor gravimetric system for the adsorption/desorption experiment. The Bigtooth Aspen chips were screened with a rotary shaker so that the chips passed through a 19 mm mesh and were removed with the 12 mm mesh screen. (The average dimensions of these chips were (16 mm x 29 mm x 5 mm, (± 2 mm))). The chips were dried at 105 °C for 2-4 days. The oven dry chips were allowed to reside in the reactor for 16-20 hours while heating the reactor surface to the predetermined set point. This step served two purposes. First, it allowed the chips to reach the desired bed temperature prior to reaction. Secondly, it allowed the Teflon lined flex tubes to relax to their new position. This eliminated a source of gravimetric drifting during adsorption/desorption loading measurements.

b. Facility Operation

The experiment was conducted on the day following the reactor loading. The objective of the experiment was to gather loading versus time data for adsorption and desorption at a predetermined set of operating conditions. The operating conditions and typical values are summarized in Table 3.

Table 3, Range of Operating Conditions Chosen Before Each Experiment

1.	Temperature	45-63 °C (same for adsorption and desorption)
2.	HF Flow Rate	10-60% of Full Scale (0.75-5.79 g/min)
3.	Final HF Loading	26-82%
4.	Initial Desorption N_2 Flow	0.75-6.00 slpm

When the operating conditions were selected, the operation of the apparatus proceeded in a straightforward manner.

The heat tracing and HF supply system were first prepared for operation by warming to a constant temperature. The HF tank heating controller was activated to gently warm the cylinder. The tubing heat tracing was turned on while a small nitrogen flow (0.5 slpm) passed through the system. The heating systems were allowed to equilibriate for 2-3 hours to eliminate unsteady temperature effects. The neutralization system was started to contain any accidental HF releases.

Following system warm up, the apparatus was prepared for HF flow. The nitrogen flow was re-routed to bypass the reactor. This prevented accidental HF introduction to the bed. The tank valve was opened 1/2 turn, and the manual and remote purge valves were placed in the "HF" position. (At this point there was no flow in the system, because the HF cannot pass through the closed manual control valve, and the nitrogen cannot pass through the purge valves.)

The HF flow began following these preparations. The manual control valve was slightly cracked to allow a trace HF flow. (Note that the HF flow will bypass the reactor.) The flow controller reading was monitored as the manual valve was opened to increase the flow. The control valve was opened until a flow 10% greater than the set point was acheived.

The system pressure was monitored as the controller acted to limit the flow. If the pressure exceeded 35 kPa, the manual control valve was closed slightly to prevent condensation. At this point, the HF tank heater was connected to a percentage controller, adjusted so that the input power was roughly equal to that required to vaporize the HF, (15-60% of full voltage). After pressure fluctuations subsided, the manual control valve was adjusted to create a backpressure of 17 kPa in the supply system.

The hood sashes were closed after the HF backpressure stabilized and the data acquisition system had been prepared for the adsorption cycle. Slight adjustments to the backpressure were made by adjusting the tank heater controller. Once the vapor temperature and flow rate had stabilized, (10-20 minutes), the flow was passed through the reactor. At this instant the data acquisition system was activated, marking the $t = 0$ point of the data. The adsorption cycle proceeded until the predetermined HF loading had been achieved.

At the end of the adsorption cycle, the vapor flow was again diverted directly to the neutralization column. The hood sashes were momentarily opened and the tank and manual control valves were closed. The remote purge valve was then positioned to allow a nitrogen flow to purge the system. All heat tracing prior to the reactor inlet heater was then turned off. The transient gas temperature fluctuations subsided within 10 minutes, after which the gas flow was passed through the reactor to begin the desorption cycle. At this moment, the data acquisition system was activated to gather the desorption gravimetric data. The desorption was continued at the original reaction temperature for 36 to 48 hours, leaving a 5-15% HF residue on the sample.

2. Reacted Sample Preparation and Extraction

The purpose of the sample extraction procedure was to provide product solubility data under different extraction conditions, and to provide solution samples for sugar yield analysis. A complete preparation and extraction procedure is given in Appendix B. It is summarized in the paragraphs to follow.

The reacted samples were removed from the reactor basket in the form of a dry, flaked black solid. The samples were held under vacuum for 24 hours to remove residual HF and remaining volatile compounds. The solid was then crushed to a flaked powder.

Weighed portions of the sample were extracted into aqueous solution at three different conditions. These conditions are summarized in Table 4.

Table 4, Extraction Conditions of HF Reacted Samples

	Extractant Mixture	Initial Solution Temperature	Conditions of Exposure
1.	10 g sample with 100 ml Distilled Water + Trace HCl	50 °C	Addition of solution heated to 50 °C, 18 hr. soaking at room temperature.
2.	10 g sample with 100 ml Distilled Water	100 °C	2 hour soaking while cooling to room temperature.
3.	2 g sample with 100 ml 3% H_2SO_4	121 °C	Autoclave at 121 °C 1 hr., 2 hr. cooling to room temperature

The purpose of the extraction 1 was to assess the fraction of the reacted solid that was soluble in water near room temperature. The boiling water extraction was used to see if temperature had an effect on product solubility. The dilute sulfuric acid post hydrolysis was used to hydrolyze any water insoluble oligosaccharides into species with higher solubility.

In all cases, the slurry was filtered through weighed #1 filter paper. The solid residues were thoroughly washed, dried at 100 °C, and weighed, as a measure of the insoluble fraction. The filtrate was diluted and saved for future HPLC analysis.

RESULTS AND DISCUSSION

A. Summary of Experimental Objectives and Operating Conditions

Several experiments were performed to accomplish the following objectives:

1. To assess the operability of the bench scale system.
2. To measure the rates of adsorption and desorption at various operating conditions.
3. To analyze the samples which were produced by each experiment.

Each experiment was conducted with a 100 g packed bed of (16 mm x 29 mm x 5 mm, (± 2mm)) Bigtooth Aspen (Populus Grandidentata) wood chips. The operating conditions for each of the eleven initial experimental runs are summarized in Table 5. The experiments were conducted at three temperatures; 45, 55, and 63 °C. The desorption cycles were conducted at the same temperature as the corresponding adsorption cycle.

The base case HF flow rate was 20 % of full scale, (full scale = 0-10 g/min nominal HF flow rate), with the actual HF flow varying from 1.23-1.56 g/min, due to the effects of HF exposure on the flow controller calibration. (Later, it will be demonstrated that these slight variations in HF flow rate had little effect on the overall adsorption characteristics.)

Table 5, Summary of Operating Parameters

Run #	Temperature °C	HF Flow Rate, g/min	Adsorption Time, Min	Final HF Loading, %	Initial N_2 Flow Rate, slpm*
1	45	0.62	28	38.5	0.75
2	45	1.48	115	49.3	0.75
3	45	1.56	180	76.1	0.75
4	45	1.53	180	82.3	0.75
5	55	1.32	180	61.5	0.75
6	63	1.30	180	40.1	0.75
7	55	1.23	105	52.0	0.75
8	55	5.79	125	45.7	6.00
9	55	0.75	156	64.2	4.00
10	55	1.30	65	40.3	0.75
11	55	1.34	25	26.2	0.75

*The initial desorption cycle proceeded for the first 100 minutes of desorption, all samples were desorbed at 0.75 slpm for the remainder of the desorption cycle.

Adsorption experiments were compared at 55 °C for three HF flow rates: 0.75, 1.32, and 5.79 g/min. Other runs at 55 °C proceeded to HF loadings of 64%, 62%, 52%, 40%, and 26%, to assess the amount of conversion achieved at sub-equilibrium loadings.

The base case nitrogen flow rate was 0.75 slpm, used for a majority of the desorption cycles. Initial one-hour desorption data for nitrogen flows of 0.75, 4.0 and 6.0 slpm at 55 °C were also obtained.

B. Adsorption Characteristics of the Bench Scale System

1. Adsorption at Moderate HF Flow Rate

The adsorption versus time data, (adsorption profiles), were measured directly with the bench scale gravimetric reaction apparatus. The repeatability of the adsorption profiles were demonstrated in runs 3 and 4, (at 45 °C); and in runs 5 and 7, (at 55 °C). Results of these experiments are presented in Figures 6 and 7. The same basic characteristics are demonstrated at both temperatures; the initial acid

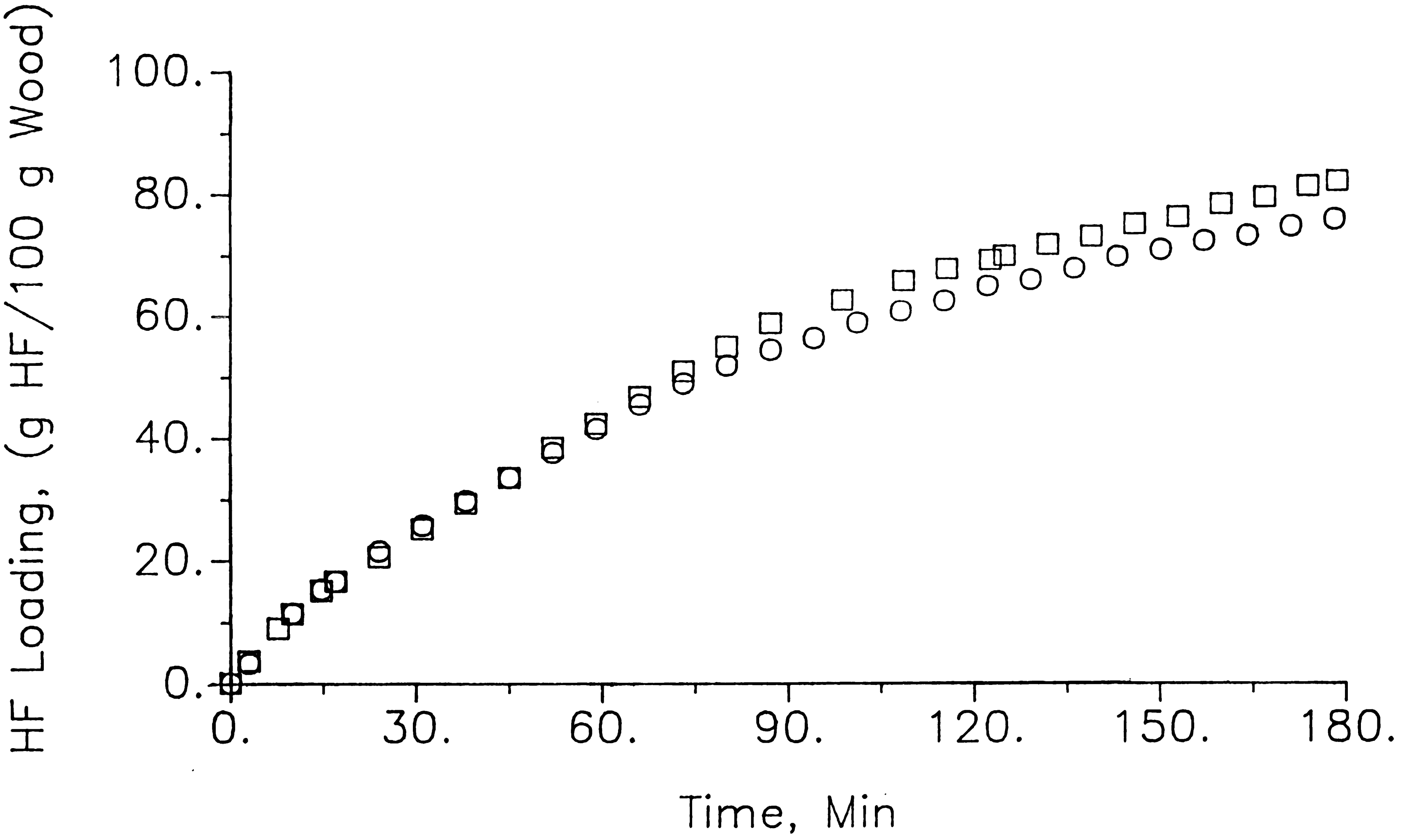

Figure 6, Repeatability of Adsorption Profile
T = 45 °C, 1.5 g HF/min

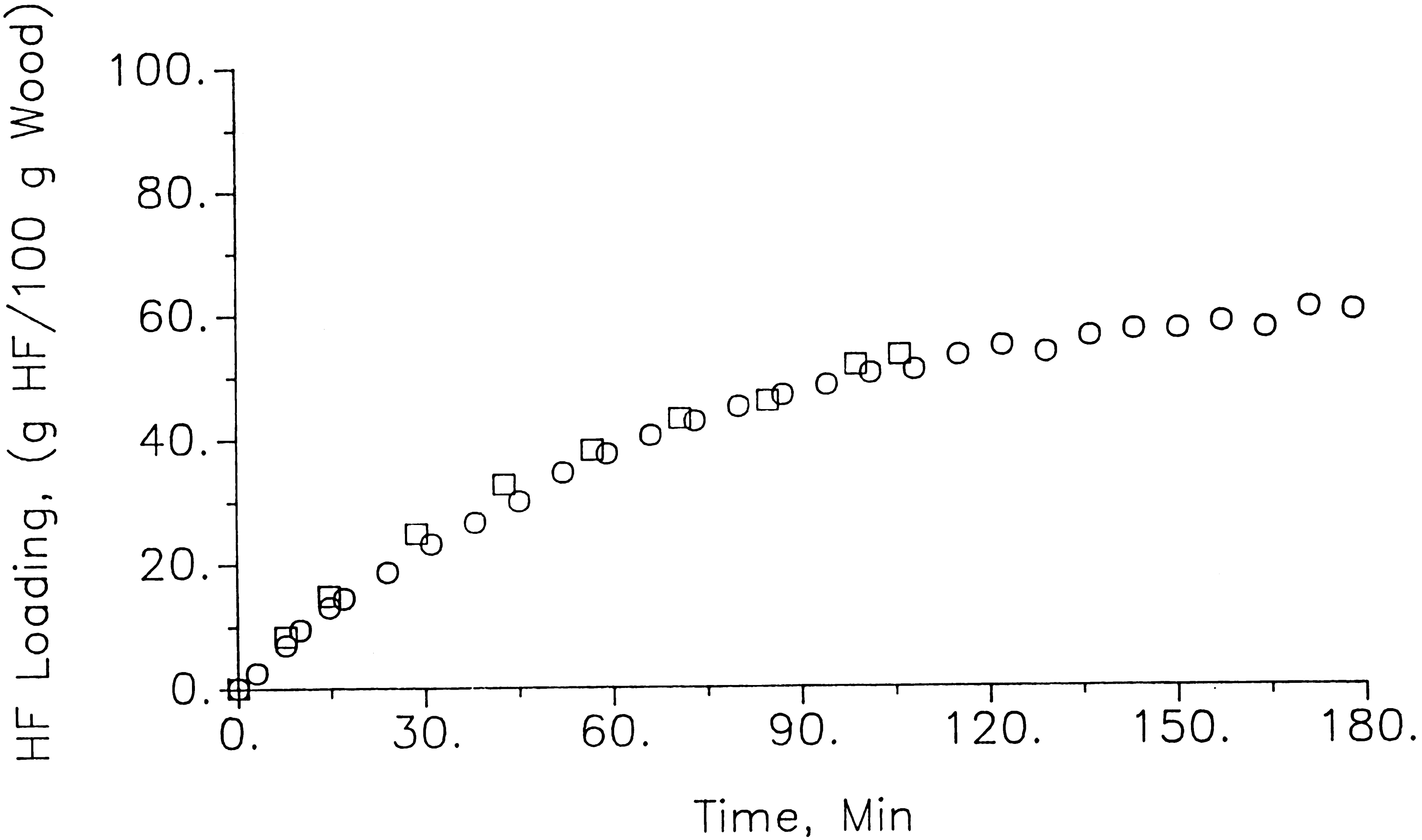

Figure 7, Repeatability of Adsorption Profile
T = 55 °C, 1.3 g HF/min

uptake is rapid, and approaches an equilibrium level after about 2.5 hours.

In Figure 6, the loading characteristics between 0 and 90 minutes are nearly the same and are reproducible to within ± 2.2g. However, a 6 g discrepancy between the two runs develops by the end of the 3 hour HF exposure. This obviously reflects differences in the equilibrium characteristics of the bed. The different equilibrium characteristics may be due to temperature measurement errors. (A temperature difference of 2 °C between the two runs will cause an eight gram difference in the equilibrium loading (from data of Mohring and Hawley, 1989).) In the bench scale system, the reaction temperature was measured indirectly; it was assumed to be equal to the reactor surface temperature. (This was based on the assumption that the vapor would reach thermal equilibrium with the reactor surface before contacting the wood.)

In Figure 7, it appears that the temperature difference between the two runs was on the order of 1 °C; runs 5 and 7 were repeatable to within ± 1.5 g at the end of 105 minutes of adsorption.

The adsorption profiles were measured at temperatures of 45, 55, and 63 °C to assess the variation of loading characteristics with temperature at the base case HF flow rate. Figure 8 presents the results of these experiments. Notice that the equilibrium loading decreases with increasing temperature. This temperature effect is quite dramatic; the equilibrium loading is reduced by a factor of two over a temperature range of 18 °C. This is similar to the temperature dependence demonstrated at the microscale by Mohring and Hawley (1989).

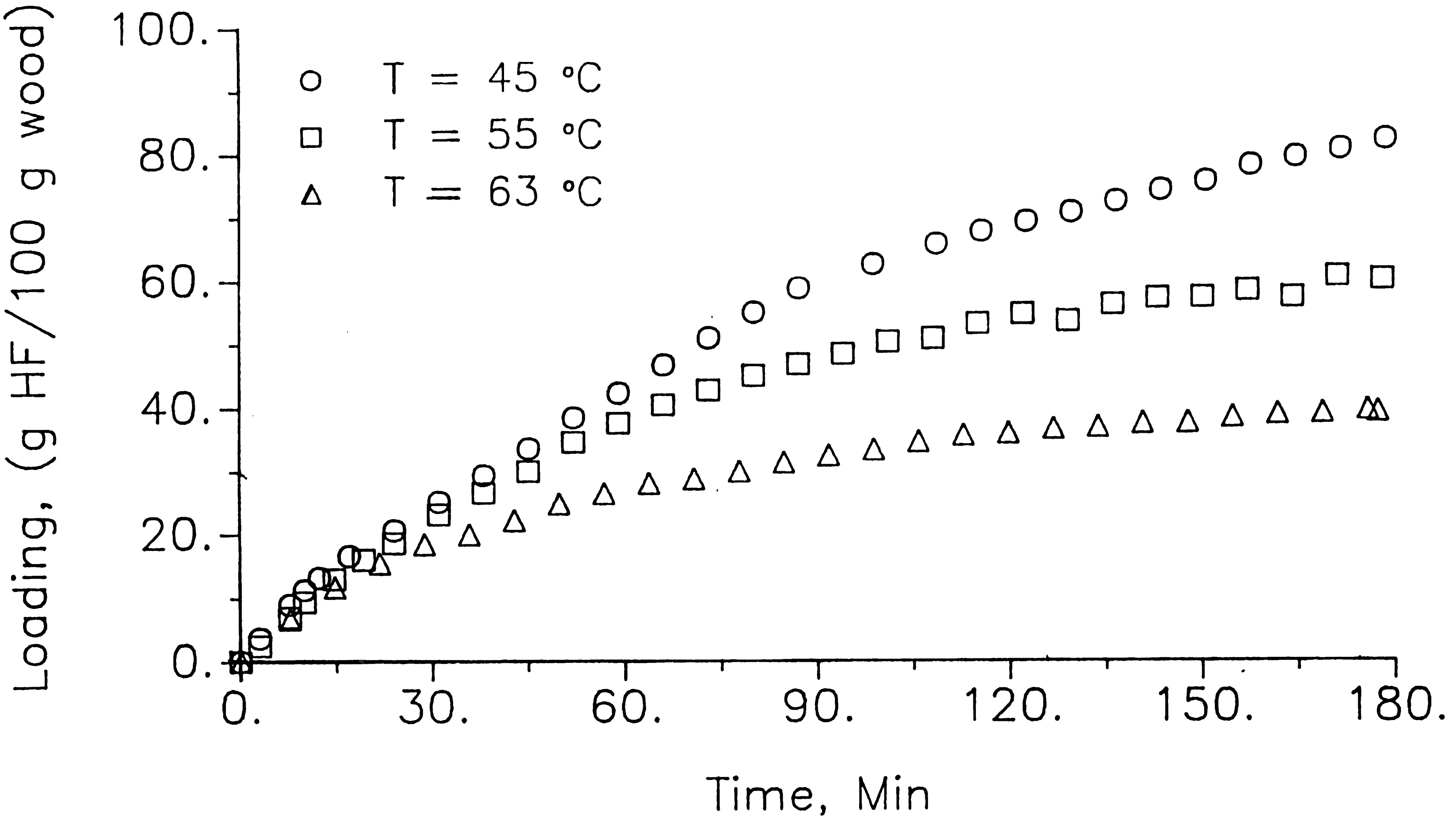

Figure 8, Effect of Temperature on the Adsorption Profile

The equilibrium loadings measured with the bench scale apparatus are compared with those measured with the microscale apparatus in Table 6. Note that in all cases the final loading in the bench scale experiments was higher than the equilibrium loading reached in the microreactor experiments.

Table 6 Comparison of Bench Scale and Microscale Final HF Loading

Temperature °C	Microreactor Equilibrium Loading, %*	Bench Scale Final Loading, %
45	73	82.3
45	73	76.1
55	49	64.2
55	49	61.5
63	35	40.1

*Data from Mohring and Hawley (1989).

The apparent difference between the bench scale and microscale equilibrium loading may be be attributed to: temperature measurement errors, HF vapor condensation, or reactor component HF absorption.

A control experiment was conducted to assess the amount of reactor vessel HF absorption. Here, the reactor was prepared identically to those used in the other adsorption experiments, except that no wood was used. The long time results of this experiment indicated that no condensation occurred in the reactor vessel. (The equilibrium level remained constant for 45 minutes.)

However, a small amount of HF was absorbed by the reactor components. At 55 °C, a 5 gram equilibrium level was attained within 15 minutes of HF exposure. This residual loading was probably due to HF absorption onto the polyethylene basket used in the reactor.

The results of the control experiment and the uncertainty of the reaction temperature measurement account for the apparent differences between the bench scale and microscale equilibrium loadings.*

2. Effect of HF Flow Rate on Adsorption

The adsorption profiles were measured at 55 °C for three HF flow rates: 0.75, 1.31, and 5.79 g/min. The data from these experiments are presented in Figures 9a and 9b. (Note that Figure 9a is a portion of the data plotted in Figure 9b, only on a shorter time scale.)

In Figure 9a, the adsorption rates during the first 5 minutes of desorption, (as given by the slopes of the adsorption profiles), have a large flow rate dependence. This may reflect a fundamental property of the pure HF reaction medium; mass transfer resistances exist only during the initial stages of the reaction, as air diffuses out of the porous substrate and forms a film at the gas-solid interface. The mass transfer coefficient will depend on flow velocity as long as the diffusion film exists.

Once the air has left the substrate, the HF concentration at the solid-gas interface is 100%, and the mass transfer film resistance is nonexistent. If this is true, latter stages of adsorption would show no dependence on flow rate, similar to that shown in Figure 9a. The slopes of the adsorption profiles after 8 minutes of exposure are nearly independent of flow rate. It must be emphasized that this will only be true for adsorption with pure HF; the film resistance will always be present if a dilutant gas is used.

---

*The reader should note that all loading profiles presented here are the actual data. No corrections for reactor component adsorption were made.

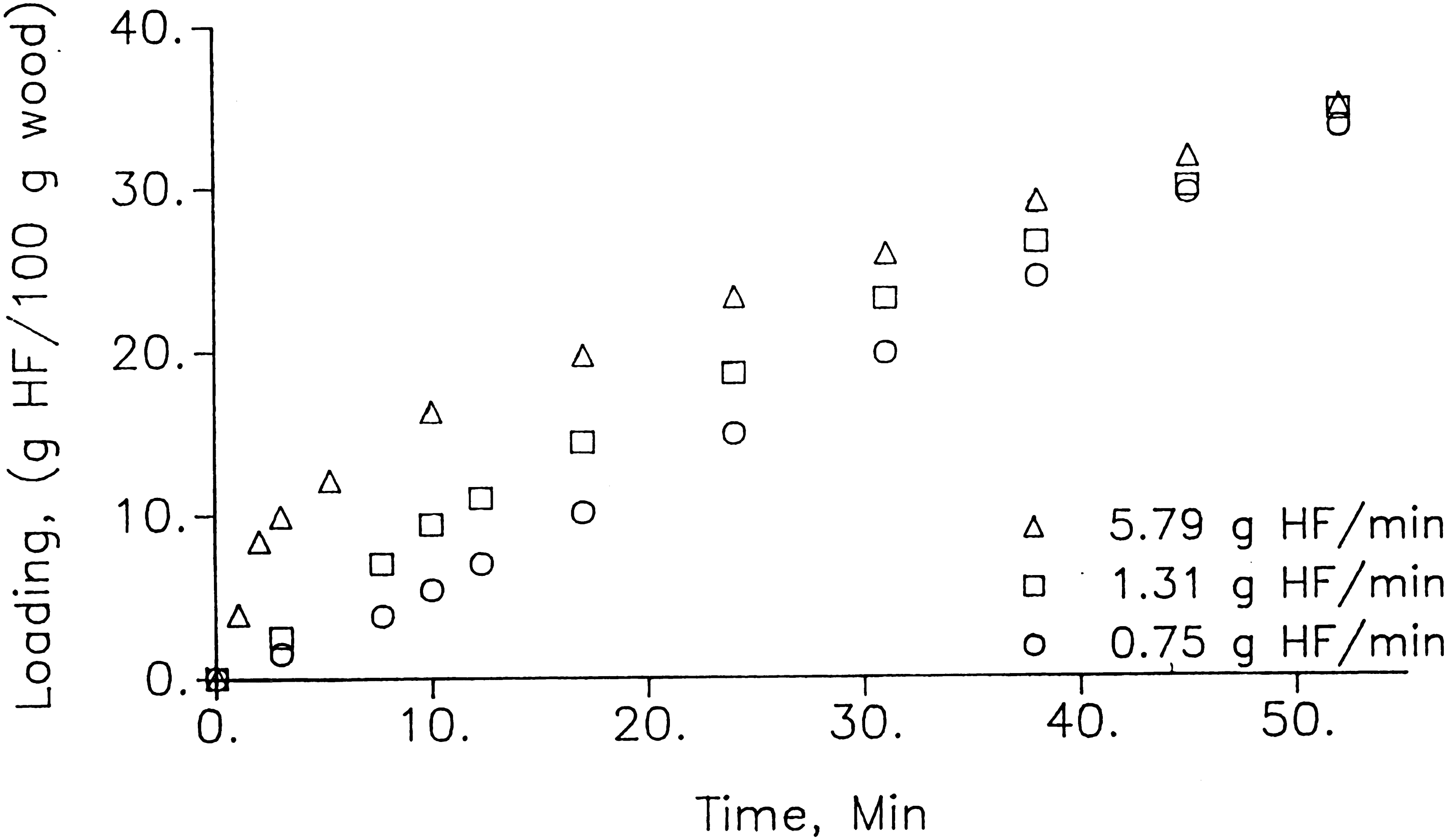

Figure 9a, Effect of HF Flow Rate on Adsorption Profile (Short Time)

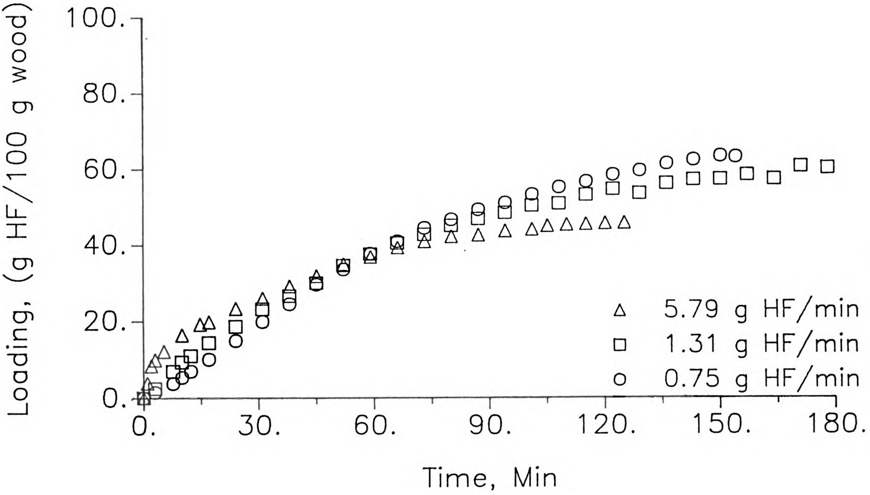

Figure 9b, Effect of HF Flow Rate on Adsorption Profile (Long Time)

Note that mass transfer effects are not the only explanation for this phenomenon; heat transfer also plays an important role in adsorption. This will be discussed in the following paragraphs.

Adsorption is a very exothermic process. Loading-dependent adsorption enthalpies in the range of 200-600 (cal/g HF) were calculated by Morhing and Hawley (1989). The exothermic nature of adsorption may also contribute to the phenomenon illustrated in Figures 9a and 9b. In the initial stages of adsorption, the particle surfaces rapidly adsorb HF. This releases heat at the gas-solid interface. The larger heat transfer coefficients present at high flow rates effectively dissipate this heat, allowing further adsorption to occur.

As adsorption continues, however, loading occurs at the interior of each particle, generating heat at the interior. Low thermal conductivity of the wood will trap much of this heat within the particle, raising the interior temperature. (This decreases the local equilibrium loading, and decreases the loading rate.) Since the heat transfer is now controlled by thermal conduction and not by by heat transfer at the gas-solid interface, the adsorption rates are independent of flow rate.

Given the large adsorption enthalpy, it is likely that heat transfer is the rate controlling step. At this point, however, we cannot conclude whether adsorption is limited by heat transfer, mass transfer or both. Future experiments using a dilutant gas will be required to measure the long time adsorption rates in the presence of mass transfer resistances. (If the adsorption rate remains independent of flow rate, then heat transfer must be rate limiting.) Unfortunately, the current configuration was unable to perform such experiments.

It is encouraging that the bench scale apparatus was able to confirm the exothermic property of adsorption, which was detected as an increase in the reactor surface temperature. In Figure 10, the reactor temperature versus time profiles are presented for three HF flow rates. The temperature profiles for the highest two flow rates exhibit a maximum after about 5-10 minutes of HF exposure. This maximum is a result of the adsorption rate decrease discussed previously. A time lag exists between the temperature profile maximum and the maximum adsorption rates due to the thermal capacity of the reactor and substrate. Although such observations are only qualitative, they suggest that calorimetric methods may be used to monitor adsorption rates in large scale commercial reactors.

One final question related to HF flow rate remains to be addressed; Is there any advantage to using increased HF flow rates during adsorption? To help answer this, a loading efficiency was defined as the ratio of the HF loading to the total amount of HF passed through the bed, as defined in equation 1:

$$E_{HF} = (L_{HF} / (M_{HF} \times t)) \times 100 \qquad (1)$$

E_{HF} - HF Loading Efficiency, (%)
L_{HF} - Current HF Loading, (g)
M_{HF} - HF Flow Rate, (g/min)
t - Time, (min)

The adsorption profiles in Figure 9b are replotted in Figure 11, in terms of loading efficiency. In spite of increased initial loading rates at higher HF flow, the loading efficiency is greatly reduced over the entire adsorption time. It is clear that little is gained at higher flow rates with pure HF.

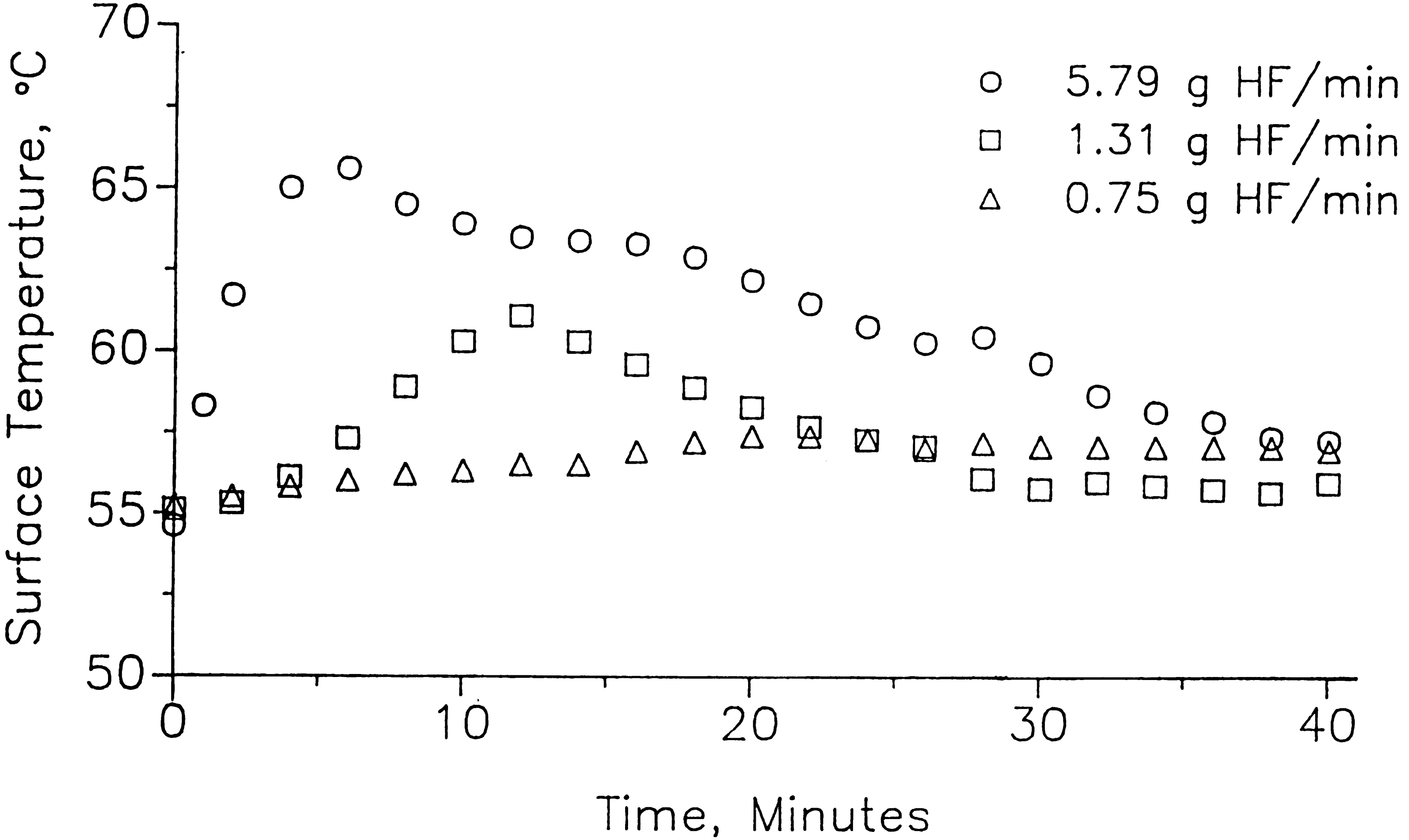

Figure 10, Effect of HF Flow Rate on Reactor Surface Temperature, T_o = 55°C

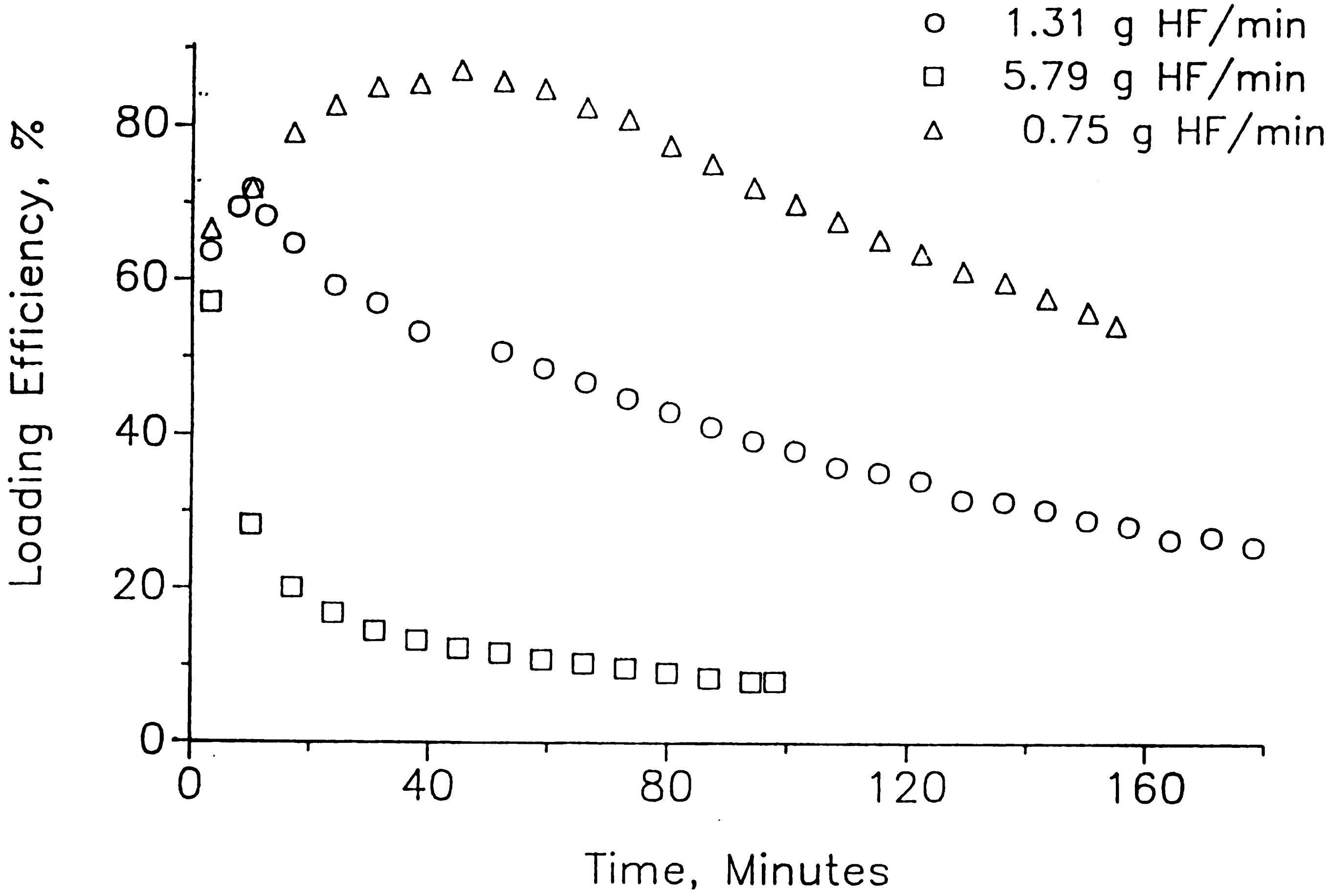

Figure 11, Effect of HF Flow Rate on Loading Efficiency

Remember that these results are limited to reactions involving pure HF. It will be interesting to see the dependence of efficiency on flow rate in the presence of a dilutant gas. If adsorption is not mass transfer limiting, the efficiency profiles should show a similar flow rate dependence.

C. Comparison of Packed Bed and Single Chip Adsorption

A single chip adsorption experiment was performed by Mohring and Hawley (1989). An 85 mg chip (10mm x 10mm x 2mm) was exposed to a 50% HF/N_2 mixture at 30°C in a microscale gravimetric apparatus. An identical experiment was performed with a thermocouple embedded in the center of the chip.

During the initial stages of adsorption, it was found that the loading profile was less than that predicted by the equilibrium loading at the center temperature. The opposite was true after a loading of 42% was achieved; the loading had risen above that predicted by the center temperature. It was concluded that this behavior was a consequence of temperature gradients within the chip.

Figure 12 compares the adsorption profile of this experiment with that obtained in packed bed reactor*. It can be seen that the single chip requires about one twelfth as much time to reach equilibrium loading. This probably reflects differences in heat transfer capabilities between the single chip and packed bed reaction configurations, as well as differences in chip size. The existence of

*The equilibrium HF loading at 30 °C and 50% HF is 62.5%; the loading measured with the packed bed at 55 °C was between 62% and 64%. The single chip experiment at 55 °C and 100% HF should show faster loading characteristics, due to decreased heat and mass transfer resistances.

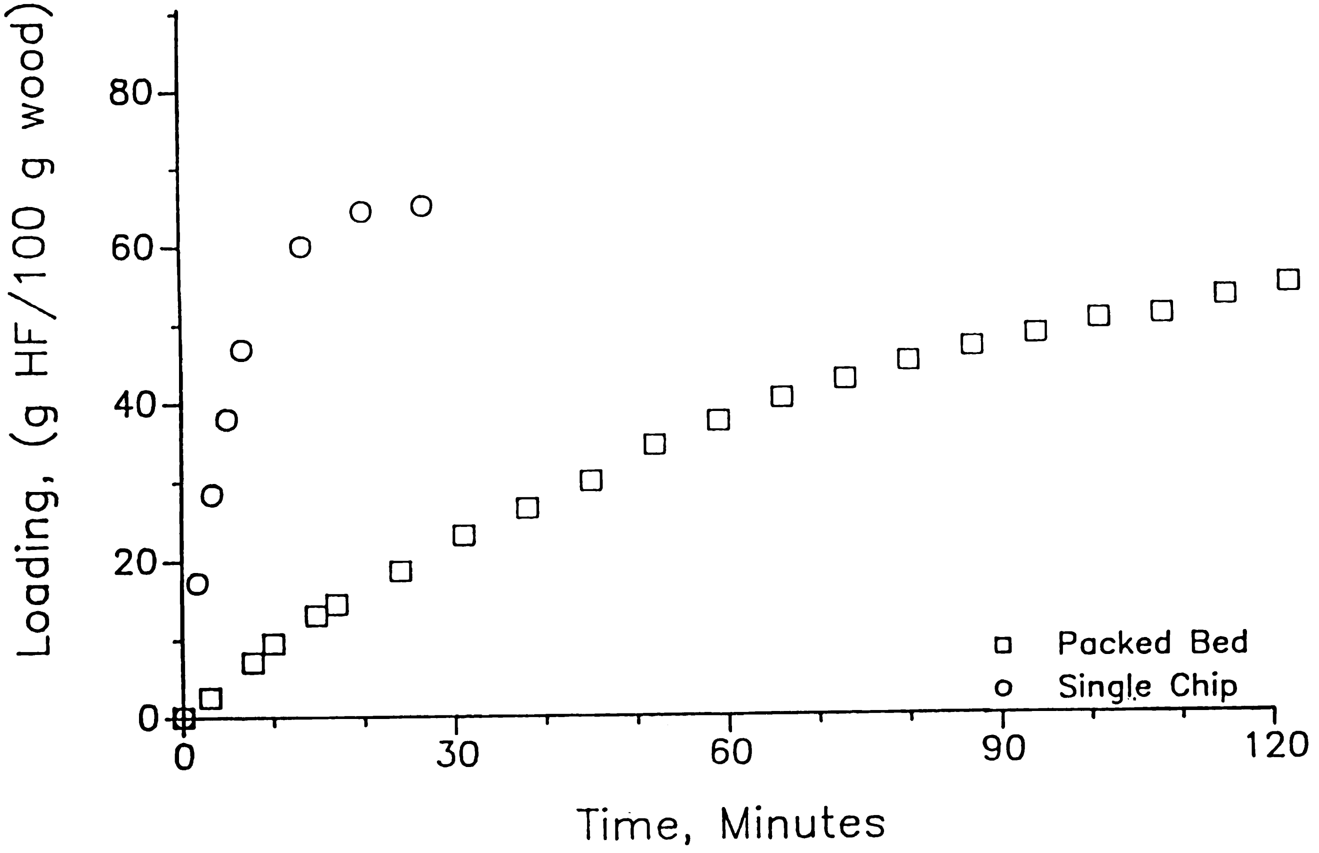

Figure 12, Comparison of Bench Scale and Single Chip Adsorption Profiles

T

po

te

temperature gradients detected in the single chip experiments would support the hypothesis that the bench scale adsorption rates are heat transfer limited. If the single chip had appreciable temperature gradients, the packed bed should have even larger temperature gradients.

However, we must be bear in mind that some fundamental differences existed between the single chip and packed bed experiments. These are:

1. Much larger chips (700 mg) were used in the bench scale reactor than in the single chip experiment (85 mg).
2. Reactions were conducted at entirely different conditions of temperature and HF partial pressure.

For these reasons, detailed comparisons between these experiments are not recommended at this point.

D. Desorption Characteristics of the Bench Scale System

1. Dependence of Desorption on Temperature

The desorption cycle is a direct consequence of the adsorption cycle, because the HF must be removed before the reactor may be safely opened and unloaded. The desorption cycle is conducted at the same temperature as the corresponding adsorption cycle. The desorption data acquisition commenced when the nitrogen carrier gas was passed through the bed. The packed bed desorption process continued until approximately 5-15% HF remained on the sample, and when an exceedingly slow desorption rate occurred (0.2 - 1.0 g HF/hr). At this point, the reaction product could be safely handled with the usual precautions. The substrate was removed from the reactor and placed into a polyethylene container for immediate frozen storage.

Figure 13 presents the desorption versus time profiles at the three temperatures studied. Rapid initial desorption rates are followed by

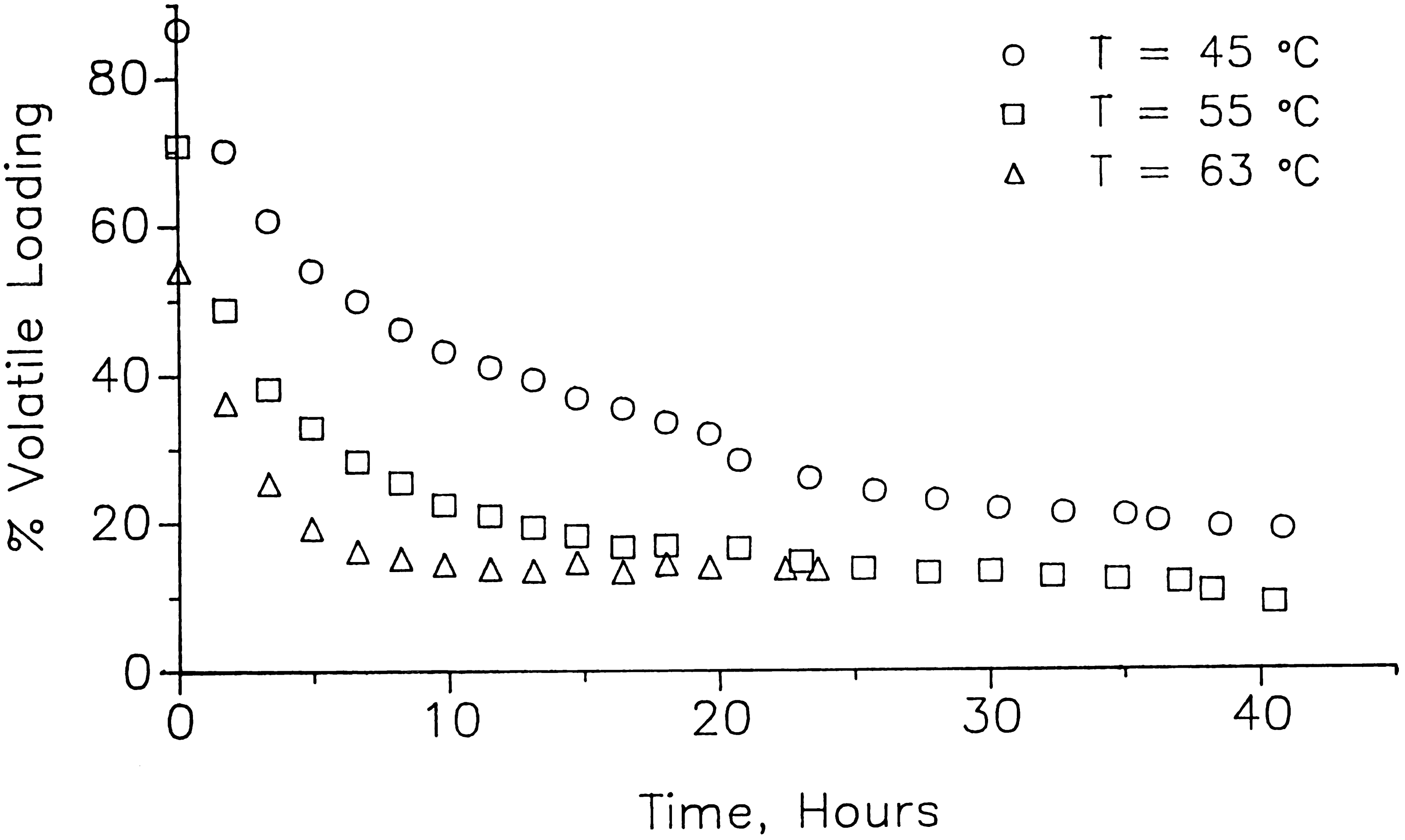

Figure 13, Effect of Temperature on Desorption Profile very slow rates in all cases studied. This is most likely due to differences in the nature of the adsorbed HF; adsorbed HF is either physically contained in the substrate, or chemically bound in the form of sugar fluorides. In the initial stages of desorption, physically contained HF is rapidly removed from the pores of the substrate. When most of this "pore" HF is removed, the desorbed HF is produced primarily by reversion of sugar fluorides into oligomers.

In Figure 13, it is interesting to note that the at t = 45 hrs the loading at 45 °C (20%) is roughly twice that at 55 °C and 63 °C. This may be an indication of the reversion rate, or may reflect differences in the structure of the reacted product. Certain mechanisms of pore collapse may trap HF within the solid, forcing it to be transferred by a chain type intermolecular exchange of fluoride and hydroxyl groups.

Mohring and Hawley (1989) performed single chip desorption measurements which indicated that at 30 °C, desorption to 5% loading occurred in the first hour; desorption to constant weight required seven additional hours. It is unclear why the packed bed desorption rates are 5-8 times slower than the single chip desorption. Factors that may contribute to this phenomenon include:

1. Larger chip size in bench scale experiments.
2. Collapse of packed bed void space, (chip settling).
3. Collapse of individual chip pore structure.
4. HF retention by lignin.
5. Lack of substrate moisture, (Prolongs the existence of sugar fluorides, with a corresponding reduction in the rate of HF regeneration.)

A study of the above factors will provide insight to the rate controlling steps that dominate desorption. Once these rate controlling steps are identified, improved desorption configurations will be designed.

2. Dependence of Desorption on Flow Rate

The initial desorption data were obtained at 55 °C for nitrogen flow rates of 0.75, 4.00, and 6.00 slpm. In each of these cases, the initial data were gathered for approximately 100 minutes at these flow rates. Folowing this initial period, the flow was reduced to from 4.00 and 6.00 slpm to 0.75 slpm for the remaining 35-48 hours of desorption.

The behavior of the initial desorption with changes in nitrogen flow rate is presented in Figure 14. From the figure, it is clear that the desorption rates are dependent on the nitrogen flow rate only during the first five minutes of desorption. This is consistent with the observation that the process is limited by heat transfer only during the high initial desorption rates. In all cases, the desorption rates after the first 10 minutes are similar, as given by the slope of the profiles.

3. Weight Characteristics of Desorbed Products

The nitrogen desorbed samples were removed from frozen storage and placed under vacuum (760 mm Hg) for 24 hours. The purpose of this treatment was to remove residual HF and other volatile compounds. This step permitted the safe handling of the samples outside of the fume hood.

The weight of the samples were recorded before HF exposure, and after vacuum desorption. The results of these measurements are presented in Table 7. The final desorbed weights of the samples, (following the 24 hour vacuum treatment), were consistently less than the initial wood charge.

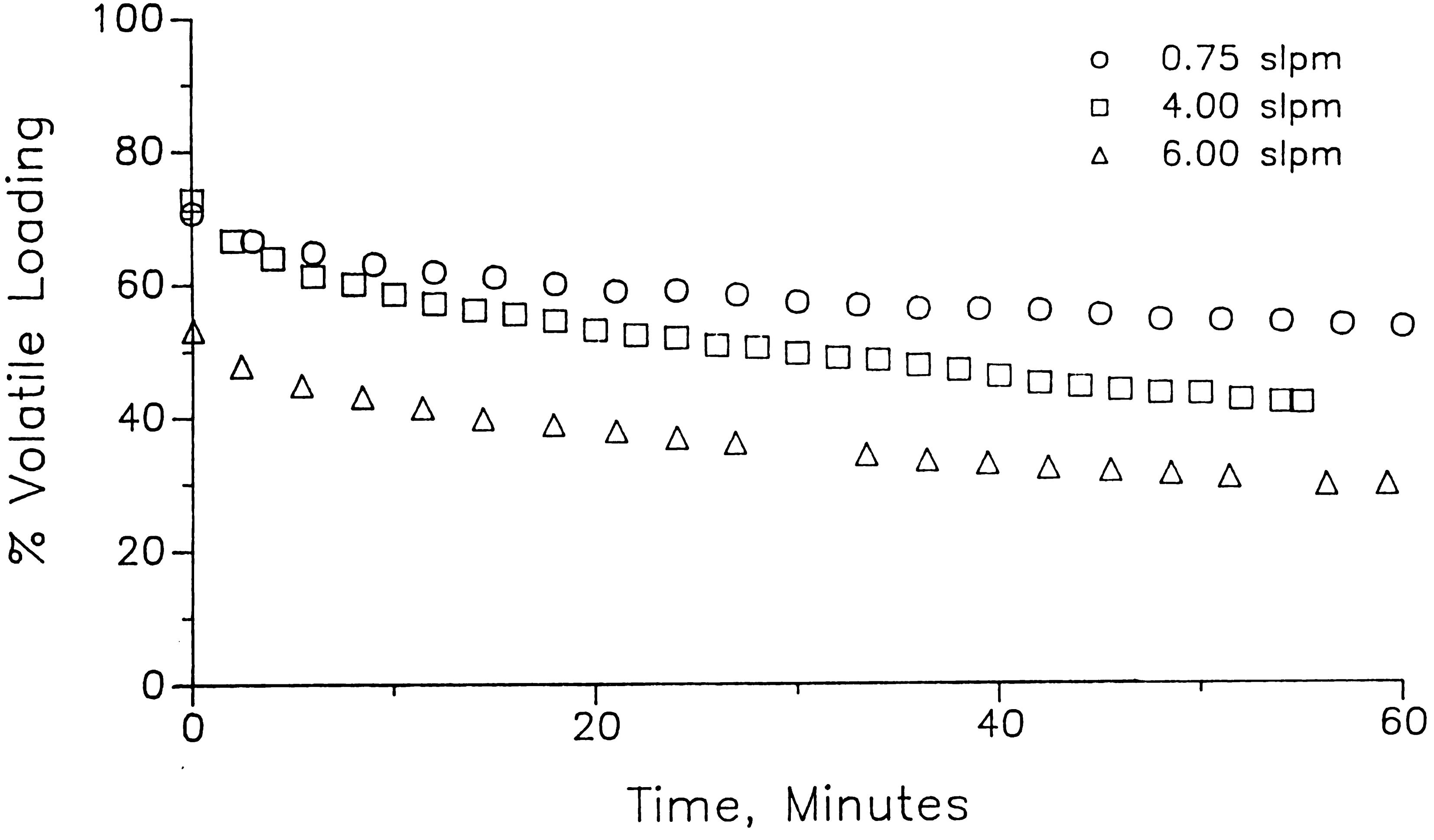

Figure 14, Effect of Nitrogen Flow Rate on Initial Desorption Profile

Table 7. Weights of Wood Charge and Final Desorbed Product

Temperature °C	Adsorption Time, Minutes	HF Loading % Wood Wt.	Initial Bed Weight, g	Desorbed Bed Weight, g
45	180	76.1	99.9	90.7
55	180	61.5	100.1	90.9
63	180	40.1	100.1	89.9
55*	156	64.2	100.2	91.7
55**	125	45.7	100.2	94.3
55	65	40.3	100.0	95.7
55	25	26.2	100.0	97.5

*HF Flow Rate = 0.75 g/min.
**HF Flow Rate = 5.78 g/min.

In most cases the total weight change was 5-11%. Visual inspection of the reactor indicated that this loss was not attributable to residues remaining in the reactor. Disassembly of the vessel following seven experimental runs revealed only a small amount (< 2g) of sugar residues in the reactor fittings. Thus, as an extreme upper limit, 1-2% of this weight loss could be attributed to product losses during handling. An additional 3% can be attributed to volatile acetyl compounds present in the wood sample (Timell, 1957). The remaining 1-6% may be the result of volatile sugar and/or lignin degradation by-products. In contrast, the microscale experiments typically produced a 3% weight loss.* Apparently, the formation of volatile by-products in the bench scale system was due to the higher temperature and longer HF exposure during adsorption and desorption, respectively.

---

* This weight loss occurred after nitrogen desorption only. The microscale samples did not use vacuum desorption to remove residual volatile compounds. The maximum loss observed for nitrogen desorbed bench scale samples was about 8 grams.

E. Appearance of the Reaction Products

The desorbed chips were removed from the reactor and several forms were observed, depending on reaction conditions and final loading. In the cases that reached equilibrium loading, (runs 3-6, 8, and 9), the chips appeared as a dense, black, shiny solid, like coal, similar to those described by Luers (Luers, 1938). In some of these cases, the original wood grain and chip size was visible, (runs 5, 6, 8, and 9), while in other cases, the samples broke into small (1.5 cm) particles (run 3). Following run 2, the bed collapsed into a rigid plug, and could be removed from the reactor as a single entity with 20 - 25% residual HF. This product was not reproducible, however. The initial packed bed had a total volume of 500 ml, while the volumes of the fully reacted samples ranged from 200-300 ml.

Lignin can be extracted with liquid HF at 0 °C in a relatively uncondensed form as a straw-colored insoluble residue (Clark, 1962). Clark (1962) found that increased extraction temperature (30 °C) produces a dark lignin residue, evidently a result of HF-induced autocondensation reactions. The results of experiments conducted by Defaye et al. (1983) suggest that lignin autocondensation reactions occur when wood was exposed to HF for longer than 30 minutes at temperatures above 0 °C. Certainly, the higher exposure temperatures, (45-63 °C), and longer exposure times, (1.5-3.0 hours), of the bench scale experiments will promote similar reactions. The dark black color of the bench scale samples probably indicates that some lignin condensation had occurred.

A five-point rating system was devised to assess the appearance of the samples. These criteria are summarized in Table 8. Note that a higher score implies a greater degree of sample degradation.

The samples were rated on their appearance before and after grinding. The appearance of the samples are summarized in Table 9. Notice that in Table 9 the samples loaded at the base case flow rate for a period longer than 2.5 hours, (runs 3, 5, 6, and 9), showed the greatest degree of sample degradation. Samples loaded to sub-equilibrium levels (less than 90% of equilibrium, runs 7, 10, and 11), generally appeared less reacted. The sample exposed to the high HF flow rate, (run 8, at 5.79 g HF/min), appeared reacted even though it was only loaded to 70% of equilibrium. This is probably due to the higher temperature experienced by this sample.

Table 8, Criteria Used to Judge Reacted Samples

(Appearance of Packed Bed)

1 - Chips only slightly reacted. Structure intact, medium brown in color. Very few corners and edges have small (2-10 mm^2) areas of black reacted solid. No volume change.

2 = Chip structure intact. Darker brown in color. Most corners and edges have black reacted surfaces. Small (< 10%) volume change.

3 - Chips almost entirely blackened. Some chips at the top of the bed have dark brown surfaces. Chip size and original grain clearly visible on all chips. Moderate (25 %) volume decrease.

4 = Chips entirely blackened. Original characteristics are visible on many chips. Some fine flaked material produced. Much of the original chips fall out of reactor basket when inverted. Approximately 40% decrease in bed volume.

5 = Chips entirely blackened, original characteristics visible on less than 10 chips. Bed will not fall out of basket when inverted. Yielded smaller, (1.5 cm) agglomerates when bed is disturbed.

(Appearance of crushed product)

1 - Impossible to crush sample. Strength of wood intact. Only 5% of sample will pass through #14 sieve.

2 - Cannot crush entire sample. Large fraction (> 50%) will flake off, crush easily, and pass through #14 sieve. Sieved material is largely fibrous, brown in color, with some black particles.

3 = Entire sample can be crushed, yielding an even mixture of black fibrous and flaked particles.

4 = Entire sample easily crushed, with majority of black flaked particles, some small fibrous particles, and some black fine powder.

5 - Entire sample easily crushed. Produces no visible fibrous particles, but some flaked particles. Majority of sample forms a fine black powder.

Table 9, Summary of Reacted Sample Appearance

Run #	Temperature °C	Adsorption Time, Min	Final Loading	Packed Bed Appearance	Crushed Appearance	Total
3	45	180	76.1	5	5	10
5	55	180	61.5	4	5	9
6	63	180	40.1	3	5	8
7	55	105	52.0	3	3.5	6.5
8	55	125	45.7	4	4	8
9	55	156	64.2	4	5	9
10	55	65	40.3	2	2	4
11	55	25	26.2	1	1	2

F. The Reacted Product Extractions

The extraction operations were conducted to assess the product solubility at three different extraction conditions. These extraction conditions were summarized in Table 4. As discussed in the experimental, the purpose of extraction 1 was to assess the solubility of the reacted product in a polar solvent near room temperature. Extraction 2 was performed to assess the effect of temperature on the water solubility of the sample. The dilute sulfuric acid treatment of extraction 3 was used to convert water insoluble oligomers into species with greater solubility, without degradation side reactions.

The results of these extractions were expressed as a percentage of the reacted sample weight that was soluble. The repeatability of the extraction was investigated with runs 3 and 5. The solubility percentage varied by approximately ± 2.5% for extraction 1. This variation is probably due to the inhomogeneity of the ground reaction product.

The extraction results are presented in Table 10. There is little difference in the solubility of the various samples, with the exception of run 10, exposed to a sub-equilibrium loading at moderate temperature for a relatively short time.

Table 10, Solubility Characteristics of Reaction Products

Run #	HF Loading/ Adsorption Time (% / minutes)	% Soluble Extraction #1 (± 2.5%)	% Soluble Extraction #2 (± 2.5%)	% Soluble Extraction #3 (± 2.5%)
3	76.1 / 180	38	37	63
5	61.5 / 180	35	33	67
6	40.1 / 180	32	34	60
7	52.0 / 105	36	30	66
8	45.7 / 125	33	33	66
9	64.2 / 156	39	38	63
10*	40.3 / 65	32	29	45

Extraction #1, 100 ml H_2O at 50 C, cooled to room temperature, 18 hours.
Extraction #2, 100 ml H_2O at 100 C, cooled to room temperature, 2 hours.
Extraction #3, 3% H_2SO_4, Autoclave at 121 °C, 1 hour, cooled to room temperature for 1.5 hours

*A 68 g portion of partially reacted sample that would pass through # 1.4 mm sieve. Figures presented reflect 68% of total solubility

These solubility differences are probably dependent on the combined effects of HF loading, temperature and exposure time. This would explain the low solubility of run 10 samples, exposed at a moderate temperature for a shorter time. It is interesting to note that runs 7 and 8, exposed at 55 °C for 100 and 125 minutes, respectively, have solubilities similar to runs 3,5, and 6, (exposed for 180 minutes). This suggests that a contact time of about 100 minutes is sufficient for adaquate sample conversion.

Extractions 1 and 2 yield similar results, probably indicating the extraction of polar compounds, not significantly affected by the water temperature. The slight decrease in the soluble fraction in extraction 2 may be due to mass transfer difficulties, and the inability of water to wet the particle surface in the relatively short contact time.

The solubility results of extraction 3 are markedly different from extractions 1 and 2, with the soluble fraction being almost twice that of the other treatments. There are two explanations for the differences in solubility.

One explanation is that hemicellulose was present in the samples following HF exposure. Hemicellulose would not be soluble in extractions 1 and 2, but would be suceptible to dilute acid hydrolysis during extraction 3. However, the entire hemicellulosic fraction of the sample, (22.4%), cannot account for the observed 25-30% solubility increase. Furthermore, it is unlikely that the hemicellulose would remain unreacted in the presence of HF at high concentrations.

A more plausible explanation is that sugar oligomers or sugar-lignin complexes were formed during HF exposure. It is possible that these compounds were insoluble in water, but were hydrolyzed to soluble species in dilute acid at 121 °C. This hypothesis is supported by similar HF-lignin carbohydrate retention reported in the literature. A lower (4%) carbohydrate retention was reported by Clark (1962). Defaye et al. (1983) demonstrated that a time- and temperature-dependent reduction in observed glucose yields was the result of carbohydrate retention. (Of the 12% yield reduction, about 9% were DMSO soluble compounds; the remainder was assumed to be lignin-bound.) A 10-15% HF-lignin carbohydrate retention was detected by Fredenhagen and Cadenbach (1933) when wood sugars were exposed to prereacted HF lignin in the presence of HF. However, vapor phase experiments conducted at 30 °C by Rorrer (1989) were unable to confirm these results.

Rorrer (1989) found that completely reacted Aspen samples produced a 22% HF-lignin insoluble residue. If there were no soluble lignin degradation products formed in the bench scale experiments, the solubility measurements indicate that 77-86 % of the wood carbohydrates were rendered soluble following post hydrolysis of the bench scale products. This is comparable to results obtained with bench scale saccharification of barley straw. (Reffstrup, 1986).

Table 11 compares the appearance rating to the solubility data. It is demonstrated in Table 11 that a high degree of lignin condensation, indicated by dark coloration, and other physical factors, is not necessarily required for high product solubility. In fact, the appearance rating system was a poor predictor of the sample solubility.

Table 11, Comparison Between Appearance Rating and Solubility Data

Run #	Total Appearance Rating	% Solubility (Extraction #3)
3	10	63
5	9	67
6	8	60
7	6.5	66
8	8	66
9	9	63
10	4	45

The results of the HPLC sugar analysis were not available at the time of this writing. The data will be incorporated into the last table of Appendix C if available before this document is bound.

G. Summary

Some of the data obtained from the bench scale experiments could be compared to those obtained from previous microscale and single chip experiments. These comparisons include:

1. Adsorption in the packed bed requires 100-180 minutes to attain adaquate sample conversion. This compares with 3-5 minutes with the microreactor experiments, and 10 minutes with the macroscopic single chip experiment. It is probable that packed bed adsorption rates are heat transfer limited.
2. The effect of temperature on equilibrium HF loading confirmed the microreactor results, when the temperature and gravimetric measurement errors are considered.
3. Desorption from the packed bed required 35-48 hours to attain a residual level of 5-15% HF. This contrasts with the 7 hours required to attain complete desorption in the single chip experiment.
4. Vacuum desorbed samples consistently weigh 5-10% less than the unreacted wood. This compares with a 3% weight loss in the microreactor experiments.

Other information was not available from the previous experiments. The following are unique observations regarding the nature of bench scale HF saccharification.

1. HF flow rate had little effect on the long-time adsorption rates. This was probably due to the internal heat transfer limitations of the substrate.
2. Nitrogen flow rate had almost no effect on the initial desorption rates. This probably indicates that bench scale desorption is not limited by external heat or mass transfer.
3. The appearance of the reaction products varied with HF exposure time, and temperature. Black appearance of fully reacted samples may indicate a high degree of lignin condensation.
4. Reaction products were about 35% water soluble at 100 °C, compared with 65% solubility in 3% sulfuric acid at 121 °C This may indicate the presence of water insoluble oligomers, or sugar-lignin complexes.

In most instances, the results of these experiments were inconclusive; one possible cause for an observed behavior could not be eliminated from another. However, the experiments demonstrated that HF can be safely adsorbed and desorbed from a macroscopic packed bed of wood chips under controlled conditions of temperature and flow rate. Considering that the current system was intended as an experimental prototype, the successful results are very encouraging. Many equipment- and environment-related difficulties were solved in the execution of the experiments; these solutions will be incorporated into future designs of inproved bench scale systems.

CONCLUSIONS AND RECOMMENDATIONS

1. Summary of Results and Observations from the Current Apparatus

The objectives of this investigation were:

1. To design and construct a gravimetric apparatus to process up to 250 grams of standard sized wood chips in a packed bed reactor.
2. To obtain HF loading versus time data for different temperatures and flow rates during adsorption and desorption.
3. To obtain reacted wood samples for visual inspection, solubility, and sugar yield analysis.

The bench scale characterization experiments successfully adsorbed and desorbed HF with a 100 gram packed bed of standard sized wood chips. HF loading versus time data were obtained for adsorption at temperatures of 45, 55, and 63 °C, and HF flow rates of 0.75, 1.31, and 5.79 g/min. Similar desorption data were obtained at 55 °C and nitrogen flow rates of 0.75, 4.00, and 6.00 slpm. The nitrogen desorbed samples were further desorbed *in vacuo* at room temperature. Weight measurements were taken before HF exposure and after vacuum treatment. The vacuum desorbed chips were extracted with three solvent systems to determine the soluble fraction.

A number of conclusions regarding the nature of HF adsorption and desorption may be drawn from the gravimetric data, solubility data and product appearance evaluations. Within the range of conditions studied, the following behavior was observed:

1. Adsorption in the packed bed requires 100-180 minutes to attain adaquate sample conversion. This compares with 3-5 minutes with the microreactor experiments, and 10 minutes with the single chip experiment. HF flow rate had little effect on the long-time adsorption rates.

2. The effect of temperature on equilibrium HF loading confirmed the microreactor results, when temperature and gravimetric measurement errors are considered.

3. Desorption from the packed bed required 35-48 hours to attain a residual level of 5-15% HF. This contrasts with the 7 hours required to attain complete desorption in the single chip experiment. Nitrogen flow rate had almost no effect on the initial desorption rates.

4. Vacuum desorbed samples consistently weighed 5-10% less than the unreacted wood. This compares with a 3% weight loss in the microreactor experiments.

5. The appearance of the reaction products varied with HF exposure time and temperature. Black appearance of fully reacted samples may indicate a high degree of lignin condensation.

6. Reaction products were about 35% water soluble at 100 °C, compared with 65% solubility in 3% sulfuric acid at 121 °C

The observation that the rates of adsorption and desorption are much slower in the bench scale than in the microscale, and the fact that these rates are unaffected by HF or nitrogen flow rate, are difficult to explain.

One plausible explanation is that packed bed adsorption is heat transfer limited. To conclusively demonstrate heat transfer effects, however, accurate bed temperature and gas stream temperature measurements are needed. A different reactor vessel is required for these measurements.

It is encouraging that the bench scale experiments confirmed the equilibrium loading characteristics measured in the microscale investigations. Improved reaction temperature measurements and temperature control will be helpful to future reactor designs. This may eliminate the slight descrepency between the bench scale and microscale equilibrium loadings.

The formation of reacted samples that weigh consistently less than the original starting material directly implies a loss of reaction products. This may be the result of volatile product degradation, or physical entrainment of sugar fluorides in the gas phase. The current apparatus is unable to properly address the product degradation issue.

The dark lignin coloration, differences in solubility, and slow desorption rates may be closely related. These characteristics may reflect a lack of substrate moisture.* A lack of moisture would favor the formation of highly ploymerized oligomers. These products are probably insoluble in water and require post hydrolysis. Furthermore, a lack of moisture would favor the existience of sugar fluorides. The lengthy exposure of lignin to sugar fluorides in the presence of HF may catalyze the formation of lignin-sugar linkages (Defaye et al., 1983). By optimizing the substrate moisture content the desorption, solubility, and lignin condensation problems may be eliminated. This issue was addressed by German researchers, (Fredenhagen & Cadenbach, 1933) who stressed the importance of regulating the substrate moisture content.

A serious limitation of the current experiment is that the reacted product shows the combined effects of adsorption and desorption. The issue of reaction rates and by-product formation require that these effects be decoupled for a conclusive analysis. Methods to address these limitations are presented in the following section.

---

*A Canadian pilot plant used chips with 5-15% moisture, and produced water soluble products, apparently with feasible desorption (Ostrovski et al. 1985).

2. Areas for Further Study, Changes to the Current Apparatus

The next generation of experiments should systematically address the following aspects important to bench scale saccharification:

1. Lack of substrate moisture and its effect on adsorption/desorption rates and primary product characteristics.
2. Development of methods to increase adsorption and desorption rates.
3. Formation of water insoluble reaction products.
4. By-product formation.
5. HF recovery and recycle.
6. Effect of HF partial pressure on adsorption/reaction rates.

The effect of substrate moisture may be addressed in the current system, after developing quantitative methods of moisture determination. The apparatus will be operated in a slightly different manner, so that the temperature and moisture content of the chips are known prior to the reaction. After loading, and before HF exposure, the wood will be completely isolated from the system to prevent moisture loss.

Improved methods of HF contacting such as rotary drum , fluidized bed, or agitated bed configurations may improve adsroption and desorption rates. These may be developed after the fundamental aspects of the reaction are understood.

The remaining objectives require that the effects of adsorption and desorption be decoupled. This will necessitate the development of different reactor configurations. One such reactor design will add a quenching option to the existing reactor. This will be designed to allow a fluid, such as water, to be injected into the reactor to effectively quench, or stop the entire reaction in progress. This reactor will permit the bed to be analyzed to assess the average conversion of the substrate. Another reactor design could incorporate a sampling option. This will permit a sample of the reactor contents to be removed after a desired loading is achieved. This sample can be immediately quenched in water to stop the reaction. This configuration has the advantage of allowing a single run of the experiment to generate a family of samples reacted to different degrees.

Gravimetric measurements may be difficult with these types of reactors. Fortunately, gravimetric measurements are not the only method for determining the substrate loading. Franz, et al. (1985) employed a continuous KOH titration scheme to analyze the reactor exit gases for HF. The HF loading could then be calculated as the difference between the inlet and outlet HF flows. Such non-gravimetric reaction systems may be easier to operate with reactor configurations that require frequent entry to the hood. Another option to determine the HF loading is to obtain a loaded sample from the reactor and immediately quench it. The HF loading could be back-calculated from a fluoride analysis of the quenching solution. A small evaporation error must be tolerated with this method.

Most importantly, these bench scale reaction configurations must be accompanied by macroscopic single particle experiments to permit synthesis of the microreactor and bench scale results. The additional single chip experiments will determine whether intraparticle heat and mass transfer play an important role in situations where external resistances are more easily characterized. Experiments conducted without external resistances will measure the maximum rates that can be obtained with an optimum reactor configuration, allowing questions of substrate size to be properly addressed.

These new investigations will permit an integration of the bench scale and microscale results. The development of a descriptive model based on these three programs will allow for accurate scale-up and realistic economic analyses.

LIST OF REFERENCES

LIST OF REFERENCES

1. Bentsen, Th. (1982). Hydrolysis of carbohydrates in straw using a hydrogen fluoride pretreatment. In A. Strub, P. Chartier, & G. Schleser (Eds.), Energy from Biomass 2nd E C Conference, (pp. 1103-1105). London: Applied Science.

2. Clark, I. T. (1962). Determination of lignin by hydrofluoric acid. Tappi, 45, 310-314.

3. Franz, R., Erckel, R., Riehm, R., Wonernle, H., & Deger H.-M. (1982). Lignocellulose saccharification by HF. In A. Strub, P. Chartier, & G. Schleser (Eds.), Energy from Biomass 2nd E C Conference (pp. 873-878). London: Applied Science.

4. Franz R., Fritsche-Lang W., Deger H.-M., Erckel R., Schlingmann M. (1985). The behavior and derivatizations of carbohydrates in hydrogen fluoride. Journal of Applied Polymer Science, 33, 1291-1306.

5. Fredenhagen K., Cadenbach G. (1933). Dissolution of cellulose by hydrogen fluoride and a new method for wood saccharification by highly concentrated hydrogen fluoride. Angewandte Chemie, 46, 113-117.

6. Gore J. (1869). On hydrofluoric acid. J Chem. Soc., 22, 396-406.

7. Luers H. (1938). The Hoch and Bohunek process for the saccharification of wood using HF. Holz Roh-Werkstoff, 1, 342-344.

8. Defaye J., Gadelle A., Papadopoulos J., & Pedersen C. (1983). Hydrogen fluoride saccharification of cellulose and lignocellulosic materials. Journal of Applied Polymer Science: Applied Polymer Symposium, 37, 653-670.

9. Defaye J., Gadelle A., & Pedersen C. (1981). Degredation of cellulose with hydrogen fluoride. In A. Strub, P. Chartier, & G. Schleser (Eds.), Energy from Biomass 1st E C Conference (pp. 319-322). London: Applied Science.

10. Hawley, M. C., Selke, S. M., & Lamport, D.T.A.(1983). Comparison of hydrogen fluoride saccharification of lignocellulosic materials with other saccharification technologies. In Energy in Agriculture, 2, (pp. 219-244).

11. Hardt H. & Lamport, D.T.A. (1982). Hydrogen fluoride saccharification of wood: lignin fluoride content, isolation of alpha-D-glucopranosyl fluoride and posthydrolysis of reversion products. Biotechnology and Bioengineering, 24, 903-918.

12. Lamport D.T.A, Hardt H., Smith G., Mohrlok S., Hawley M. C., Chapman R., & Selke S. M. (1981). HF saccharification: the key to ethanol from wood?. In A. Strub, P. Chartier, & G. Schleser (Eds.), Energy from Biomass 1st E C Conference, (pp. 292-297). London: Applied Science.

13. Mohring W. R., & Hawley M. C. (1989). Gravimetric analysis of hydrogen fluoride vapor absorption by bigtooth aspen wood. Industrial Engineering Chemistry Research, 28, 237-243.

14. Ostrovski, C. M., Aitken, J. C., Free, D., & H. E. Duckworth, (1984). Canertech's ethanol from cellulose program. In S. Hasnian (Ed.), Fifth Canadian Bioenergy R&D Seminar, London: Elsevier Applied Science.

15. Ostrovski, C. M., Aitken, J. C., & Hayes, R. D., (1985). Hydrolysis of poplar wood using hydrofluoric acid for the production of ethanol. In D. L. Klass (Ed.), Energy from Biomass and Wastes IX, 895-914. The Institute of Gas Technology: Chicago.

16. Reffstrup T., & Kau M. (1985). Hydrogen fluoride-aided hydrolysis of lignocellulosic biomass: Development of a fast continuous process. In R. Hill, & L. Munk, (Eds.), New Approaches to Research on Cereal Carbohydrates, (pp. 313-317). Amsterdam: Elsevier Applied Science.

17. Reffstrup, T. (1986). Saccharification of straw by means of a continuous hydrogen fluoride pretreatment. Meddelelser fra Bioteknisk Institut, A. T. V, Afdelinger for Bioteknologi, Symposium on the Pretreatment of Lignocellulosic Materials, June 23-24, 1986.

18. Rorrer, G. L., Ashour, S. S., Hawley, M. C., & Lamport, D.T.A. (1987). Solvolysis of wood and pure cellulose by anhydrous hydrogen fluoride vapor. Biomass, 12, 227-246.

19. Rorrer, G. L., Hawley, M. C., & Lamport, D.T.A. (1986). Reaction rates for gas-phase hydrogen fluoride saccharification of wood. Industrial Engineering Chemistry Product Research and Development, 25, 589-595.

20. Rorrer, G. L., Mohring, W. R., Hawley, M. C., & Lamport, D.T.A. (1988). Adsorption and reaction processes of the solvolysis of wood and pure cellulose by anhydrous hydrogen fluoride vapor. Journal of Energy and Fuels, 2, 556-566.

21. Rorrer, G. L., Mohring, W. R., Lamport, D.T.A., & Hawley, M. C. (1988). A detailed kinetic and heat transport model for the hydrolysis of lignocellulose by anhydrous hydrogen fluoride vapor. Chemical Engineering Science, 43, 1831-1836.

22. Rorrer, G. L. (1989). Solvolysis of a single lignocellulose particle by anhydrous hydrogen fluoride vapor: reaction rate studies, sugar yield studies, and development of a detailed kinetic and heat transport model. PhD Dissertation, Department of Chemical Engineering, Michigan State University, East Lansing, Michigan. (in press).

23. Selke S. M., Hawley M. C., Hardt H., Lamport D. T. A., Smith G., & Smith J. (1982). Chemicals from wood via HF. Industrial Engineering Chemistry Product Research and Development, 21, 11-16.

24. Timell, T. E. (1957). Carbohydrate composition of ten North American species of wood. Tappi, 40, 568-572.

25. Wenzl, H. F. J., (1970). Summative wood analysis. In The Chemical Technology of Wood (F. E. Brauns & D. A. Brauns, Trans.), (pp. 95-101). Academic Press: New York.

APPENDICES

APPENDIX A, DETAILS OF APPARATUS DESIGN AND CONSTRUCTION

1. Tubing Sizes, Valves and Fittings

The plumbing prior to the HF flowmeter consisted exclusively of 6.3 mm Monel tube and fittings. This posed no pressure drop difficulties, even at high flow rates, because a high system pressure exists at this point. The remainder of the system, with exception of the valve assemblies, consisted of 9.5 mm Monel tubing, to minimize pressure drop. The 9.5 mm tube and fittings formed a very rugged assemblies, capable of withstanding a variety of torques during construction and repairs. In future applications requiring free standing tube assemblies, 9.5 mm tube is highly recommended. Some of the fittings required for the system were only available in carbon steel. These fittings showed almost no evidence of corrosion, and were capable of reassembly following 15 hours of HF exposure. However, in future applications involving moisture exposure, only Monel and teflon fittings should be used.

The valves in the system have Monel and Kel-F wetted parts, to ensure continued precise operation. The valves were selected to minimize pressure drop through the apparatus. These valves were only available for use with 6.3 mm tubing, requiring the creative use of various conversion assemblies. The teflon lined tubing may be assembled with a 9.5 mm fitting at one end and a 6.3 mm fitting on the other. The use of 9.5 mm-6.3 mm conversion fittings were thus minimized by combining the a flexible tube with a tubing size reduction in a single assembly.

2. Vessels of the System

The top of the reactor was constructed from 7.6 cm PVC pipe fittings. This is not recommended in future designs, as this material is difficult to heat without inducing dimensional changes. The reactor wall was assembled of 3.1 mm thickness copper tube. Originally, copper was selected to permit vessel heating and facilitate desorption. In retrospect, the use of copper had little effect on desorption, and was not absolutely required. Clearly other materials may be preferred, especially if water contact is expected to occur. If a polymer, such as teflon, is employed, care must be taken to specify fittings with very coarse threads, as fine teflon threads are easily stripped. The reactor was designed to eliminate all HF leakage. Any reactor design should be capable of withstanding pressures of at least 100 kPa. Small leaks, (100 ml/hr) are impossible to detect at the low system operating pressures. These leaks are soon discovered by the HF, however. The reactor basket was hand-constructed from protective mesh screen obtained from the McMaster-Carr Corporation in Chicago.

The neutralization system is well represented in the thesis text. The column was constructed from 15 cm sch 80 PVC pipe, with 1.03 MPa flange fittings. The polypropylene fittings attached to the vessel were 12 mm NPT or larger, to prevent thread stripping. The fittings used with the plastic tubing were a Parker brand compression type available from the United States Plastic Corporation, Lima Ohio*. These fittings worked exceptionally well, with no detectable liquid leakage. The 12 mm polyethylene rashig rings were obtained from Universal Plastics in

---

* This company is also an excellent source of other handy plastic products.

Akron, Ohio. The circulation pump is a magnetic drive vane pump, designed for low pressure systems. The use of standard drive pumps is strongly discouraged because these can generate high pressures if dead ended, causing complete system failure. The caustic pumps were never employed, because direct tank caustic mixing was more convenient. If these are used in the future, an inlet screen must be employed to prevent solids from entering and damaging the pumps. Originally, these pumps were intended for use in an automatic titration system. Such a system may prove to be an effective method to detect desorption rates.

3. Heating of the System Components

Heating of the system is absolutely necessary to prevent any HF condensation. Condensation causes erratic flow controller operation and destroys the purge valves. All precautions must be employed to guard against possible condensation.

Heating the system in the well ventilated hood environment proved challenging during the initial construction. The tubing was wrapped with standard heating cord at a frequency of about 2.54 cm per revolution. The heated tubing of the entire system was wrapped with heat-resistant 3-M aluminum tape so that the it was more evenly heated. Bare thermocouples were glued to the tube at important locations to verify the operation of the heating systems. The mass flowmeter were similarly wrapped and heated to 45-60 C. Conversation with Matheson representatives verified that this is well within the operating temperature range of the controller. Only the electronics must be kept below 50 C. All heat tracing required about 5-30% of full input power to maintain adequate temperatures. The heat tracing broke down frequently, but was easily repaired with clamping type electrical connectors and electrical tape. It is recommended that a higher quality tracing be found from an industrial supply company.

The heating connections consumed about 28 amperes of current, requiring the use of extension cords to prevent circuit overload. The calculation of electrical consumption was absolutely necessary to determine the load on each electrical supply circuit. It is recommended that future laboratory installations have at least 60 amperes of supply current located near the apparatus.

4. Reactor Lift System

A pneumatic lift system was constructed to enable the reactor and tank to be raised from the balances. The air cylinders were each capable of lifting over 20 kg with an air pressure of 345 kPa. These were also obtained from the McMaster-Carr Company. The use of a similar system is highly recommended to enable maintenance of the HF tank and reactor. The existing system will serve as a prototype for future designs. In future applications, the balance platforms should be constructed from aluminum. The wood platforms used in this study warped slightly after three months of service.

5. The HF Flow Controller

A Matheson model 8203 flow controller with a nominal flow range of 0-10 g/min was used for these experiments. The factory calibration was apparently an average of the HF conditions expected for the instrument. The calibration of the controller varied with backpressure and flow rate. For this reason, a continuous monitor of the flow rate will be required in future systems, unless precautions are taken to ensure that the temperature and backpressure are identical from run to run. A corrosive gas pressure regulator may be an excellent addition to the system, to maintain a constant system backpressure, and is highly recommended, (Matheson sells one for under $500.).

The flow controller was used to indicate leakage in the system. A final on/off valve, installed prior to the neutralization column, was closed during pressure testing. The entire system was pressurized to 100 kPa with nitrogen. The flowmeter was then isolated from other systems by positioning the purge valves halfway between "purge" and "flow" settings. The system was allowed to sit for 30-60 minutes. Locations of very small flow leaks can be deduced by observing the flowmeter response as isolated portions of the system are reconnected to the flowmeter. A leak prior to the flowmeter will cause a momentary decrease in the reading, while a leak after the flowmeter will cause a momentary increase in the reading. The flowmeter is a very useful leak detector when used creatively. Trust its readings.

6. The Data Acquisition System

The data acquisition system has three basic components, an IBM-PC/XT microcomputer, Omega OM-815 A/D, D/A, Digital I/O, interface board, and the RS-232 balance serial interface. The thermocouple voltage was conditioned with Omega thermocouple to analog converters. The linearized thermocouple signal, (0-300 mv) was connected in full differential mode to the interface board. In future applications, shielded cables should be used for all thermocouple connections, as considerable noise was generated when non shielded cable was used.

Extended serial interface cables were constructed based on those purchased from the manufacturer. The balance programming was accomplished in straightforward manner, by following manufacturer instruction manuals.

The Labtech Notebook software package was used in conjunction with the data acquisition hardware. This is a versatile program and enabled data to be gathered and recorded in standard ASCII format. The data was gathered in the form of 7 point clusters, each point taken at a 1 Hz frequency. A software averaging function was used to average the cluster. The averages were stored every 20 seconds for adsorption and every 60 seconds for desorption. The HF tank and reactor data averages were also displayed with the real-time graphics capability of the software. This gave a continuous monitor of the controller calibration and HF loading profile. The data files were averaged using a third order least squares averaging algorithm. The averaged data is listed in Appendix C.

7. Improvements to the System

There are a number of improvements that should be made to the current system without changing the original packed bed reactor configuration.

There were some of temperature measurement difficulties. In future applications, the reactor inlet gas temperature should be measured at the immediate entrance to the reactor. The current system measured the temperature before the gas entered the teflon lined tubing that was connected to the reactor. This configuration adds uncertainty to the temperature measurement, as the vapor may cool or warm as it passes through the 100 cm tube assembly. Thermocouple probes no larger than

1.6 mm in diameter should be used for any gas stream temperature measurement; sufficient ventilation is not available at low gas flows to accurately measure the vapor temperature. The probe should have at least 7.5 cm insertion in the vapor streams. The heated tubing and fittings can cause heat conduction errors if the insertion length is too short.

The current reaction system was placed on a table 100 cm in height. This made the top of the reactor about 200 cm from the floor, so that reactor loading and unloading operations were difficult. A shorter table should be used, especially if personnel shorter than 183 cm are to use the experiment. It is necessary to inspect the loaded reactor before HF adsorption to assure that channelling will not occur. During unloading, a tool[*] was used to dislodge the reactor basket from the reactor surface; this operation was required because the reactor basket adhered to the reactor (from sugar residues or plastic melting). These operations required access above the reactor, and the author had to stand within the hood (with gas mask) to perform them

Slight changes to the reactor to permit chip temperature measurements should be made. Small thermocouple probes may be inserted into selected chips and the rest of the bed packed around them. One problem with this variation is that the internal reactor basket cannot be used to contain the chips. The internal bed temperature is a crucial measurement for reaction modeling, however, and these problems are worth solving.

[*] This tool was fabricated from a used 30.5 cm hacksaw blade with the teeth removed. This thin piece of metal was slipped between the reactor and basket to free the basket.

APPENDIX B, EXPERIMENTAL PROCEDURES AND SYSTEM OPERATION RECORD

1. Procedure for Bench Scale Operation

Prior the to execution of the experiment, the following operating parameters are chosen: Temperature, HF and nitrogen flow rate, wood loading, final HF loading.

One day before experiment:

1. Lift reactor platform from balance.
2. Weigh reactor basket and wood chips, record weights separately.
3. Place basket into reactor. Be sure that the basket makes good contact with the entire reactor wall. Leave about 500 ml dead space at bottom of reactor.
4. Lower reactor platform onto balance.
5. Turn on reactor flex tubing heaters and reactor surface temperature controller.
6. Set reactor temperature controller to desired temperature (45-63 °C).
7. Add about 800 g KOH to 50 gallon neutralization tank. Record the amount added.

Day of Experiment

1. Connect the HF tank to temperature controller. Set controller to 28-30 °C.
2. Turn on all heat tracing to low settings.
3. Set reactor inlet temperature controller to desired set point (45-63 °C).
4. Start the circulation pump at 10 l/min
5. Begin a slow nitrogen purge to bypass the bed (0.75 slpm).

6. After temperatures have stabilized, check tubing temperature with mounted and hand held thermocouples to verify heat tracing operation.

7. Adjust heat tracing controllers to until a temperature of 45-55 C is maintained in the system.

8. Allow system to stabilize for 1.5 hours.

9. Test the data acquisition system for proper operation. This is done by operating the software program and verifying the stored data.

10. Disconnect the HF tank heater from PID controller and connect to percentage controller set so that the following power is dissipated by the tank heater:

    .75 g/min ~ 45 W
    1.3 g/min ~ 95 W
    5.8 g/min ~ 175 W

    Note: If HF flow cannot begin soon after the controller is connected, it can be set to a very low setting to prevent overheating.

11. Increase tube heat input by 10% on tubing section prior to the reactor flex tubing. This will handle the added heat load of the HF flow.

12. Verify that the remote purge is in the purge position, and that the remote reactor bypass valve is in the bypass position.

13. Open hood sashes only enough to permit access to manual purge, control, and tank valves. Use sash as a protective shield.

14. Open HF tank valve 1/2 turn, control valve 1/8 turn, and position manual purge valve to connect the HF tank. At this point, a small amount of HF is flowing.

15. Close hood sashes. Activate the remote purge valve to permit HF flow. Watch the pressure gauge and flow controller readings. Do not allow the HF backpressure to exceed 35 kPa to prevent condensation.

16. Open sashes slightly and carefully adjust the manual control valve until controller indicates a flow about 10% above the set point. This is to start controller operation.

17. Watch controller reading. If controller does not respond to the flow error and reduce the flow, momentarily switch controller to closed position. This apparently permits the valve to move freely.

18. After controller begins to regulate flow, adjust manual control valve so that 17 kPa backpressure is maintained.

19. Close hood sashes and monitor backpressure flow, and HF tank temperature. Maintain constant backpressure and tank temperature with fine adjustments to the tank heat controller.

20. After inlet temperature and flow rate has stabilized, activate the remote reactor bypass valve to permit flow through the reactor. Simultaneously start the data acquisition system. Adsorption cycle begins at this point.

21. Periodically monitor HF backpressure, controller reading, inlet temperature, reactor temperature, for indication of system problems, such as equipment malfunction, leaks, and improper backpressure.

22. After the predetermined loading is achieved, return the remote reactor bypass valve to the bypass position, and stop the data acquisition system. HF flow now bypasses the reactor.

23. Open hood sashes and position all manual valves to stop HF flow. Position manual purge valve to permit nitrogen flow. Adjust flow controller to different setting if necessary, such as the base case nitrogen flow of 0.75 slpm.

24. If HF dwell time is desired, allow loaded substrate to sit for the desired dwell time.

25. Turn off all heat tracing prior to the reactor inlet heater. Allow nitrogen temperature to stabilize at 45-63 ^{o}C, (10-15 min), while preparing data acquisition software for desorption cycle.

26. After temperature has stabilized, activate remote reactor bypass valve to permit nitrogen flow through reactor. Simultaneously begin data acquisition software.

27. Allow desorption to proceed for 35 - 48 hours, until reactor weight change is equal or greater than the sample HF loading.

28. When desorption is complete, turn off all heating, use remote lift system to lift reactor, open reactor and remove sample basket. Place entire sample and basket into weighed 2 liter polyethylene container. Weigh and record weight of reacted sample, reactor basket and polyethylene container. Place container into freezer for storage.

Notes:

The flow rate of 1.3-1.6 g/min was easily maintained with the 0-10 g/min flowmeter at a backpressure of 17 kPa. The flow of 0.75 g/min was also easy to maintain, but a backpressure of 3.5 kPa was required. This is a result of the flow characteristics of the control valve. The low backpressure was used for this flow rate to permit a greater range of control valve movement, for more accurate flow control.

The flow rate of 5.78 g/min was much more difficult to maintain. This is due to the high heating rate required for this HF boiling rate. Due to the unsteady tank temperature and level, (1/3 of the tank volume was consumed in this run), the flow rate varied from 6.3 to 5.6 g/min during the course of the experiment. Such high flow rates are not recommended for use with the 1.5 Kg tank. A larger tank, with a heated water bath should be used for high flow rates.

2. Procedure for Reacted Product Extraction

Note: Steps 1-6 are used for all extractions.

1. Remove sample and reactor basket from the freezer. Allow to warm to room temperature. Separate basket from reacted sample. Place reacted sample in weighed 50 x 100 crystallization dish. Weigh and record initial sample and dish weight.
2. Place 4 such samples in 250 mm vacuum desiccator. Start vacuum pump. Allow vacuum pump to operate for 2 hours. Stop pump and allow samples to desorb for additional 22 hours.
3. After 22 hour desorption, allow dried air to slowly repressurize desiccator.
4. Open desiccator, remove samples, weigh and record the final weight.
5. Grind samples with 150 mm mortar and pestel. Transfer ground samples to 250 ml plastic centrifuge bottle.
6. Place all processed samples in vacuum desiccator with desiccant to remove residual water. Allow samples to desiccate under vacuum for 24 hours.

For Extraction #1:

1. Weigh ~ 10 g portions to .01 g and place into 250 ml plastic beaker.

2. Add 100 ml distilled water heated to 50 ½C. Add 5 drops of 1 M HCl, mix thoroughly, and allow sample to soak for 18 hours.

3. Wash and Filter sample with through #1 filter paper. Place cake into weighed petri dish. Dry filter cake at 100 C for 4 hours. Allow cake to cool in desiccator. Weigh and record weight of cake, filter paper, and petri dish. Calculate change in sample weight.

4. Dilute filtrate to 500 ml. Transfer 2 ml aliquots into plastic sample vials for future chromatographic analysis.

For Extraction #2:

1. Weigh ~ 10 g portions to .01 g and place into 250 ml plastic beaker.

2. Add 100 ml boiling distilled water. Mix thoroughly, and allow sample to soak for 1-1.5 hours.

3. Wash and Filter sample with through #1 filter paper. Place cake into weighed petri dish. Dry filter cake at 100 C for 4 hours. Allow cake to cool in desiccator. Weigh and record weight of cake, filter paper, and petri dish. Calculate change in sample weight.

4. Dilute filtrate to 500 ml. Transfer 2 ml aliquots into plastic sample vials for future chromatographic analysis.

For Extraction #3:

1. Weigh ~ 2 g portions to .01 g and place into 250 ml erlenmeyer.

2. Add 100 ml 3 wt % sulfuric acid, and mix thoroughly. Autoclave samples at 121 C for 1 hour.

3. Allow samples to cool at room temperature for 1.5 hours.

4. Wash and Filter sample with through #1 filter paper. Place cake into weighed petri dish. Dry filter cake at 100 C for 4 hours. Allow cake to cool in desiccator. Weigh and record weight of cake, filter paper, and petri dish. Calculate change in sample weight.

5. Dilute filtrate to 500 ml. Transfer 10 ml aliquots into plastic sample vials for future chromatographic analysis.

3. Notes on the HPLC Sugar Analysis Procedures

As mentioned in the text, the results of the HPLC sugar distributuion analyses will be included in the last table of Appendix C if they are available before the binding of this document. A thorough description of the analysis procedures are presented by Rorrer, (1989). The reader should consult this reference for further information.

Table 12. Adsorption Data for Runs 2-11

Adsorption Data File
Run #2, T = 45 C, HF Flow Rate = 20% of Full Scale

Time, Min (seconds)	HF Tank Weight (grams)	Reactor Weight (grams)
1.5	11679.2	11550.5
60.0	11677.5	11552.9
120.0	11675.3	11552.5
360.0	11669.3	11556.9
600.0	11662.7	11559.7
900.0	11655.1	11563.2
1200.0	11648.2	11566.5
1500.0	11640.4	11569.8
1800.0	11633.1	11573.8
2100.0	11625.2	11575.7
2400.0	11617.9	11579.3
2700.0	11609.9	11581.5
3000.0	11603.8	11584.5
3300.0	11596.0	11586.4
3600.0	11589.2	11588.0
3900.0	11581.0	11589.8
4200.0	11574.0	11591.4
4700.0	11562.4	11593.9
5000.0	11554.5	11594.8
5200.0	11550.5	11594.9
5600.0	11539.7	11596.8
5920.0	11533.4	11597.1
6340.0	11522.8	11597.7
6740.0	11513.0	11598.9
7260.0	11503.0	11599.6
7400.0	11501.9	11598.5
7460.0	11503.0	11600.4

Table 12, continued

Adsorption Data File
Run #3, T = 45 C, HF Flow Rate = 20% of F. S.

Time, Min (minutes)	Reactor Surface T (celsius)	HF Tank Weight (grams)	Reactor Weight (grams)	Calculated HF Loading (g), or %
0.0	48.8	11688.5	11479.5	0.0
3.0	45.7	11684.5	11482.8	3.3
6.0	52.7	11679.3	11487.0	7.5
9.0	59.3	11674.9	11490.5	11.0
12.0	60.6	11669.6	11492.7	13.2
18.0	56.5	11660.1	11497.0	17.5
24.0	58.9	11649.4	11501.0	21.5
30.0	52.0	11639.6	11504.4	24.9
36.0	56.8	11630.5	11507.7	28.2
42.0	51.1	11620.8	11511.3	31.8
48.0	50.3	11611.3	11515.1	35.6
54.0	48.1	11602.0	11518.1	38.6
60.0	51.6	11592.5	11521.4	41.9
66.0	46.6	11583.0	11525.0	45.5
73.0	49.3	11571.6	11528.4	48.9
79.0	49.6	11562.4	11530.6	51.1
84.0	46.3	11555.1	11532.5	53.0
89.0	45.9	11546.9	11534.3	54.8
98.0	44.6	11533.0	11537.5	58.0
104.0	46.2	11523.7	11538.9	59.4
110.0	46.0	11514.3	11540.7	61.2
116.0	46.7	11505.2	11542.5	63.0
122.0	48.6	11496.4	11544.4	64.9
128.0	49.4	11487.3	11545.4	65.9
134.0	52.0	11477.4	11547.1	67.6
140.0	51.3	11468.3	11547.9	68.4
146.0	44.8	11458.9	11549.6	70.1
152.0	50.8	11449.6	11551.1	71.6
158.0	46.7	11440.9	11551.9	72.4
164.0	47.4	11431.7	11552.7	73.2
170.0	50.7	11421.9	11554.0	74.5
176.0	43.3	11412.5	11554.9	75.4
179.3	43.2	11408.0	11555.7	76.2

Table 12, continued

Adsorption Data File
Run #4, T = 45 C, HF Flow Rate = 20% of F. S.

Time, Min (minutes)	Reactor Surface T (celsius)	HF Tank Weight (grams)	Reactor Weight (grams)	Calculated HF Loading (g), or %
0.0	45.0	11389.6	11565.2	0.0
3.0	49.8	11384.9	11568.9	3.7
6.0	52.3	11379.8	11572.3	7.1
9.0	54.4	11375.1	11575.4	10.2
12.0	57.4	11370.0	11578.2	13.0
18.0	55.7	11360.2	11582.2	17.0
23.0	54.7	11352.3	11585.4	20.2
28.0	54.5	11344.3	11588.5	23.3
33.0	54.2	11337.2	11591.4	26.1
38.0	54.1	11329.4	11594.5	29.3
43.0	52.9	11321.5	11597.5	32.3
48.0	50.7	11314.1	11600.6	35.4
53.0	51.4	11306.6	11603.7	38.5
58.0	49.1	11298.1	11607.2	42.0
63.0	48.3	11290.8	11610.5	45.3
68.0	49.4	11283.6	11613.4	48.1
73.0	49.0	11276.7	11616.1	50.9
78.0	47.7	11268.6	11619.0	53.8
83.0	46.5	11261.2	11621.7	56.5
88.0	46.7	11253.6	11624.0	58.7
98.0	45.9	11239.6	11628.4	63.2
108.2	45.2	11223.4	11630.8	65.6
118.2	46.3	11208.3	11633.6	68.4
128.2	45.6	11193.6	11635.5	70.2
138.2	45.4	11178.0	11638.2	73.0
148.2	46.0	11164.1	11640.4	75.2
158.2	44.8	11148.2	11643.1	77.9
168.2	44.8	11133.5	11645.3	80.1
178.2	45.9	11118.3	11647.0	81.8
178.5	45.3	11117.8	11647.2	82.0

Table 12, continued

Adsorption Data File
Run #5, T = 55 C, HF Flow Rate = 20% of F. S.

Time, Min (minutes)	Reactor Surface T (celsius)	HF Tank Weight (grams)	Reactor Weight (grams)	Calculated HF Loading (g), or %
0.0	55.2	11112.6	11559.1	0.0
3.0	54.4	11107.1	11561.6	2.5
6.0	58.2	11103.3	11563.6	4.5
9.0	58.0	11099.2	11566.5	7.4
12.0	61.4	11095.4	11569.8	10.6
15.0	59.5	11090.9	11571.8	12.7
18.0	59.3	11087.3	11574.8	15.6
20.0	58.3	11084.4	11575.6	16.5
25.0	57.5	11077.9	11578.6	19.4
30.0	56.6	11070.9	11581.2	22.1
35.0	54.7	11066.2	11584.4	25.3
40.0	56.2	11059.5	11587.0	27.9
45.0	55.7	11053.1	11589.0	29.9
50.0	54.2	11046.5	11591.9	32.8
55.0	54.7	11039.9	11594.9	35.8
60.0	55.7	11033.7	11597.0	37.9
65.0	55.8	11027.2	11598.3	39.2
70.0	53.6	11021.3	11599.6	40.5
75.0	54.5	11013.8	11602.7	43.6
80.0	53.8	11007.2	11604.1	45.0
85.0	55.2	11001.0	11604.6	45.5
90.0	55.5	10994.3	11607.1	48.0
95.0	53.9	10987.4	11607.4	48.3
100.0	54.6	10981.4	11608.3	49.2
105.0	53.4	10974.5	11609.3	50.2
110.0	54.1	10968.4	11610.3	51.2
120.0	54.5	10955.0	11612.5	53.4
130.0	53.7	10941.6	11614.7	55.6
140.0	54.9	10929.2	11613.5	54.4
150.0	55.1	10915.6	11616.4	57.2
170.0	53.3	10889.4	11618.2	59.1
178.0	55.1	10879.2	11619.1	60.0
179.3	53.5	10877.8	11618.8	59.7

Table 12, continued

Adsorption Data File
Run #6, T = 63-65 C, HF Flow Rate = 20% of F. S.

Time, Min (minutes)	Reactor Surface T (celsius)	HF Tank Weight (grams)	Reactor Weight (grams)	Calculated HF Loading (g), or %
0.0	63.1	10853.8	11542.1	0.0
3.0	65.1	10849.0	11545.0	2.8
6.0	67.1	10845.0	11547.8	5.6
9.0	70.2	10841.5	11550.0	7.9
12.0	68.7	10837.4	11552.0	9.9
15.0	67.5	10833.6	11554.2	12.0
20.0	67.1	10827.2	11557.0	14.8
25.0	65.4	10820.8	11559.2	17.1
30.0	67.5	10814.3	11560.7	18.6
35.0	65.9	10807.6	11562.0	19.9
40.0	65.6	10800.9	11563.9	21.8
45.0	67.0	10794.6	11565.1	23.0
50.0	67.0	10788.0	11566.8	24.7
55.0	65.1	10781.4	11568.2	26.0
60.0	65.7	10774.9	11568.9	26.8
65.0	66.7	10769.2	11569.9	27.7
70.0	67.4	10762.4	11571.3	29.2
75.0	64.3	10755.3	11571.6	29.5
80.0	67.2	10749.0	11572.9	30.8
85.0	66.4	10742.2	11573.5	31.4
90.0	65.0	10735.4	11574.1	32.0
95.0	66.2	10729.2	11574.5	32.3
100.0	65.7	10722.7	11575.5	33.3
110.0	65.1	10710.0	11576.9	34.7
120.0	66.0	10697.1	11577.9	35.8
130.0	65.0	10684.3	11578.8	36.7
140.0	66.9	10671.6	11579.8	37.7
150.0	63.9	10658.1	11579.6	37.5
160.0	66.0	10645.1	11580.5	38.4
170.0	64.0	10631.9	11581.0	38.8
179.3	66.0	10620.3	11581.3	39.2

Table 12, continued

Adsorption Data File
Run #7, T = 55 C, HF Flow Rate = 20% of F. S.

Time, Min (minutes)	Reactor Surface T (celsius)	HF Tank Weight (grams)	Reactor Weight (grams)	Calculated HF Loading (g), or %
0.0	55.0	12921.3	11193.6	0.0
3.0	55.6	12916.9	11196.5	2.9
6.0	56.8	12913.3	11199.8	6.2
9.0	60.6	12909.5	11203.5	9.8
12.0	63.4	12906.1	11205.9	12.2
15.0	62.4	12902.0	11208.8	15.1
20.0	61.7	12896.0	11213.0	19.4
25.0	59.5	12889.7	11216.1	22.5
30.0	57.9	12883.9	11217.7	24.1
35.0	56.4	12877.4	11222.2	28.5
40.0	56.2	12872.2	11224.5	30.9
45.0	54.5	12865.4	11227.2	33.5
50.0	56.0	12859.6	11229.1	35.4
55.0	54.8	12852.9	11231.3	37.6
60.0	55.6	12847.3	11231.9	38.3
65.0	54.9	12841.3	11235.7	42.0
70.0	56.2	12834.5	11237.3	43.7
75.0	55.2	12828.5	11239.1	45.5
80.0	54.6	12822.2	11239.2	45.5
85.0	55.3	12816.4	11239.6	45.9
90.0	56.0	12810.2	11242.0	48.3
95.0	54.7	12803.9	11244.7	51.1
100.0	54.8	12797.9	11245.7	52.0
105.0	54.6	12794.4	11246.8	53.1

Table 12, continued

Adsorption Data File
Run #8, T = 55 C, HF Flow Rate = 60% of F. S.

Time, Min (minutes)	Reactor Surface T (celsius)	HF Tank Weight (grams)	Reactor Weight (grams)	Calculated HF Loading (g), or %
0.0	54.3	12596.8	11519.3	0.0
3.0	64.6	12578.0	11529.2	9.9
6.0	64.6	12558.5	11532.0	12.7
9.0	65.1	12539.2	11535.0	15.8
12.0	63.9	12520.9	11536.6	17.4
15.0	63.0	12502.7	11538.4	19.2
20.0	62.2	12472.4	11540.4	21.2
25.0	60.3	12441.8	11543.0	23.8
30.0	59.8	12411.8	11544.6	25.4
35.0	59.0	12382.6	11546.7	27.4
40.0	57.9	12353.4	11548.7	29.5
45.0	56.9	12324.1	11551.0	31.7
50.0	56.4	12295.6	11553.0	33.8
55.0	56.3	12266.9	11554.8	35.6
60.0	56.8	12239.0	11556.5	37.3
65.0	56.7	12211.0	11557.9	38.6
70.0	56.9	12181.6	11559.2	40.0
75.0	56.7	12152.7	11560.2	41.0
80.0	56.3	12125.9	11561.3	42.1
85.0	55.6	12098.8	11562.3	43.0
90.0	56.2	12071.7	11562.6	43.3
95.0	56.7	12045.5	11562.6	43.4
98.0	55.7	12041.8	11562.5	43.2
101.0	55.7	12011.8	11563.3	44.0
105.0	55.9	11991.3	11564.2	44.9
110.0	56.2	11967.2	11564.5	45.2
115.0	55.5	11942.4	11564.7	45.2
120.0	56.5	11919.0	11564.9	45.6
125.0	56.3	11895.6	11565.0	45.7

Note: The HF flow rate Given in the text, 5.79 g/min, was the average flow rate for the first 98 minutes of adsorption. As can be easily seen, the flow rate varied considerably for the entire run.

Table 12, continued

Adsorption Data File
Run #9, T = 55 C, HF Flow Rate = 10% of F. S.

Time, Min (minutes)	Reactor Surface T (celsius)	HF Tank Weight (grams)	Reactor Weight (grams)	Calculated HF Loading (g), or %
0.0	55.1	11939.5	11518.8	0.0
3.0	55.6	11936.9	11520.3	1.5
6.0	56.3	11935.3	11521.8	3.0
9.0	56.6	11932.0	11523.5	4.6
12.0	56.4	11930.7	11525.6	6.7
15.0	56.6	11928.5	11527.9	9.0
18.0	56.9	11926.2	11530.2	11.4
20.0	57.3	11924.4	11530.7	11.9
25.0	57.1	11920.8	11534.8	16.0
30.0	57.6	11916.8	11537.5	18.7
35.0	57.0	11912.6	11541.1	22.2
40.0	56.8	11909.3	11544.9	26.1
45.0	56.8	11905.5	11548.3	29.5
50.0	56.9	11901.6	11551.3	32.4
55.0	57.5	11898.2	11554.3	35.4
60.0	57.1	11893.9	11557.3	38.4
65.0	56.2	11890.3	11558.6	39.8
70.0	56.0	11886.3	11561.6	42.8
75.0	56.1	11882.8	11563.3	44.5
80.0	56.1	11879.1	11565.5	46.6
85.0	56.9	11875.4	11567.2	48.3
90.0	56.1	11871.7	11568.6	49.8
95.0	56.3	11867.7	11570.3	51.4
100.0	56.2	11864.2	11572.3	53.5
105.0	56.8	11860.6	11573.3	54.5
110.0	56.2	11856.7	11574.7	55.8
115.0	56.0	11853.0	11575.4	56.6
120.0	55.9	11849.4	11577.2	58.4
125.0	56.0	11846.0	11578.1	59.2
130.0	56.0	11841.6	11579.2	60.4
135.0	56.0	11837.7	11579.7	60.9
140.0	56.3	11834.1	11581.3	62.5
145.0	56.2	11830.8	11581.7	62.9
150.0	56.1	11826.9	11582.1	63.3
155.0	56.0	11823.3	11582.0	63.1
155.3	55.9	11823.2	11581.9	63.1
155.7	56.0	11822.9	11582.3	63.4
156.0	56.6	11822.2	11583.2	64.3

Table 12, continued

Adsorption Data File
Run #10, T = 55 C, HF Flow Rate = 20% of F. S.

Time, Min (minutes)	Reactor Surface T (celsius)	HF Tank Weight (grams)	Reactor Weight (grams)	Calculated HF Loading (g), or %
0.0	55.0	11841.7	11588.3	0.0
3.0	57.2	11838.0	11591.2	2.9
6.0	57.5	11833.5	11595.2	6.9
9.0	59.8	11829.7	11598.7	10.4
12.0	61.1	11825.9	11601.2	12.9
15.0	61.7	11821.8	11604.0	15.7
18.0	61.3	11817.9	11606.8	18.5
20.0	61.8	11815.2	11607.7	19.4
25.0	60.6	11808.6	11611.4	23.1
30.0	59.0	11802.1	11614.2	25.9
35.0	57.5	11795.7	11616.8	28.5
40.0	57.1	11789.6	11619.2	30.9
45.0	57.1	11781.9	11621.5	33.2
50.0	57.5	11776.3	11623.3	35.0
55.0	56.8	11769.6	11625.3	37.0
60.0	57.4	11763.4	11627.1	38.8
65.0	57.2	11757.3	11628.6	40.2

Table 12, continued

Adsorption Data File
Run #11, T = 55 C, HF Flow Rate = 20% of F. S.

Time (Seconds)	Reactor Surface T (Celsius)	HF Tank Weight (grams)	Reactor Weight (grams)
1.5	53.9	11766.9	11583.1
120.0	55.4	11764.4	11584.4
240.0	54.9	11761.8	11587.5
360.0	56.2	11759.2	11589.9
520.0	57.5	11755.2	11592.6
600.0	58.0	11753.4	11595.0
700.0	58.4	11750.9	11596.6
800.0	57.5	11749.7	11598.7
900.0	57.3	11746.6	11601.0
1000.0	57.8	11744.5	11601.6
1200.0	57.9	11740.4	11605.7
1400.0	57.4	11735.7	11607.2
1500.0	57.5	11733.4	11609.3

Table 13. Desorption Data for Runs 3,5, and 6

Desorption Data File
Run #3, T = 45 C, N_2 = 0.75 slpm

Time (hours)	Reactor Weight (g)	Volatile Loading (g) or %
0.0	11556.8	86.6
0.9	11546.1	75.9
1.7	11540.2	70.0
2.5	11535.2	65.0
3.3	11530.8	60.6
4.1	11527.4	57.2
4.9	11524.1	53.9
5.8	11522.0	51.8
6.6	11520.0	49.8
7.4	11517.8	47.6
8.2	11516.2	46.0
9.0	11514.8	44.6
9.8	11513.2	43.0
10.6	11512.0	41.8
11.5	11511.1	40.9
12.3	11510.5	40.3
13.1	11509.4	39.2
13.9	11508.3	38.1
14.7	11506.9	36.7
15.5	11506.8	36.6
16.4	11505.5	35.3
17.2	11504.8	34.6
18.0	11503.6	33.4
18.8	11502.4	32.2
19.6	11502.0	31.8
20.4	11500.8	30.6
20.7	11498.4	28.2
23.3	11496.0	25.8
24.5	11494.9	24.7
25.7	11494.2	24.0
26.8	11493.3	23.1
28.0	11493.0	22.8
29.2	11492.3	22.1
31.5	11491.3	21.1
32.7	11491.2	21.0
35.0	11490.9	20.7
36.2	11490.1	19.9
37.3	11490.0	19.8
38.5	11489.3	19.1
39.7	11489.4	19.2
40.8	11488.9	18.7
43.2	11487.6	17.4
44.3	11485.5	15.3

Table 13, continued

Desorption Data File
Run #5, T = 55 C, N_2 = 0.75 slpm

Tim (hours)	Reactor Weight (g)	Volatile Loading (g) or %
0.0	11624.3	70.7
0.9	11608.2	54.6
1.7	11602.3	48.7
2.5	11595.6	42.0
3.3	11591.7	38.1
4.1	11588.7	35.1
4.9	11586.4	32.8
5.8	11583.4	29.8
6.6	11581.8	28.2
7.4	11580.3	26.7
8.2	11578.9	25.3
9.0	11577.0	23.4
9.8	11575.9	22.3
10.6	11574.9	21.3
11.5	11574.4	20.8
12.3	11573.8	20.2
13.1	11572.8	19.2
13.9	11572.1	18.5
14.7	11571.6	18.0
15.5	11570.5	16.9
16.4	11570.1	16.5
17.2	11570.6	17.0
18.0	11564.7	16.7
19.5	11567.7	16.7
20.7	11567.3	16.3
21.8	11566.2	15.2
23.0	11565.5	14.5
24.2	11564.3	13.3
25.3	11564.5	13.5
26.5	11561.2	13.2
27.7	11560.9	12.9
31.2	11560.6	12.6
33.5	11560.4	12.4
34.7	11560.0	12.0
35.8	11559.0	11.0
37.0	11559.6	11.6
38.2	11558.4	10.4
39.3	11558.0	10.0
40.5	11556.8	8.8
41.7	11554.0	6.0
42.8	11552.2	4.2
44.0	11552.0	4.0

Table 13, continued

Desorption Data File
Run #6, T = 63 C, N_2 = 0.75 slpm

Time (hours)	Reactor Weight (g)	Volatile Loading (g) or %
0.0	11584.7	53.9
0.9	11571.6	40.8
1.7	11566.9	36.1
2.5	11559.7	28.9
3.3	11556.0	25.2
4.1	11552.6	21.8
4.9	11549.9	19.1
5.8	11548.0	17.2
6.6	11546.8	16.0
7.4	11546.4	15.6
8.2	11545.8	15.0
9.0	11545.2	14.4
9.8	11545.0	14.2
10.6	11545.3	14.5
11.5	11544.4	13.6
12.3	11544.3	13.5
13.1	11544.1	13.3
13.9	11545.0	14.2
14.7	11545.2	14.4
15.5	11544.5	13.7
16.4	11543.9	13.1
17.2	11544.5	13.7
18.0	11545.0	14.2
18.8	11545.0	14.2
19.6	11544.5	13.7

Table 14. Initial Desorption Data for Runs 5,8, and 9

Desorption Data File, (Initial Rate)
Run #5, T = 55 C, N_2 = 0.75 slpm

Time (hours)	Reactor Weight (g)	Volatile Loading (g) or %
0.0	11624.3	70.6
3.0	11620.2	66.5
6.0	11618.4	64.7
9.0	11616.7	63.0
12.0	11615.5	61.8
15.0	11614.7	61.0
18.0	11613.7	60.0
21.0	11612.6	58.9
30.0	11611.0	57.3
39.0	11609.9	56.2
42.0	11609.7	56.0
45.0	11609.1	55.4
48.0	11608.3	54.6
51.0	11608.2	54.5
54.0	11608.0	54.3
57.0	11607.5	53.8
60.0	11607.2	53.5

Table 14, continued

Desorption Data File, (Initial Rate)
Run #8, T = 55 C, N_2 = 6.00 slpm

Time (hours)	Reactor Weight (g)	Volatile Loading (g) or %
0.0	11567.9	53.0
2.4	11562.6	47.7
5.4	11559.7	44.8
8.4	11557.9	43.0
11.4	11556.3	41.4
14.4	11554.6	39.7
17.9	11553.7	38.8
21.0	11552.7	37.8
24.0	11551.8	36.8
26.9	11550.9	36.0
33.4	11549.1	34.2
36.4	11548.3	33.4
39.4	11547.8	32.9
42.4	11547.1	32.2
45.5	11546.7	31.8
48.5	11546.2	31.3
51.4	11545.7	30.8
56.2	11544.5	29.6
59.2	11544.6	29.7

Table 14, continued

Desorption Data File, (Initial Rate)
Run #9, T = 55 C, N_2 = 4.00 slpm

Time (hours)	Reactor Weight (g)	Volatile Loading (g) or %
0.0	11591.7	73.3
1.0	11588.0	69.6
2.0	11585.6	67.2
3.0	11584.1	65.7
4.0	11583.0	64.6
5.0	11581.9	63.5
6.0	11580.3	61.9
8.0	11579.1	60.7
10.0	11577.6	59.2
12.0	11576.2	57.8
14.0	11575.2	56.8
18.0	11573.6	55.2
20.0	11572.2	53.8
25.0	11570.4	52.0
30.0	11568.7	50.3
35.0	11566.9	48.5
40.0	11565.2	46.8
45.0	11563.5	45.1
50.0	11562.6	44.2
55.0	11561.2	42.8

Table 15. Initial and Desorbed Gravimetric Data

Run #	Initial Sample Weight, (g)	Nitrogen Desorbed Weight(g)	Vacuum Desorbed Weight, (g)
2	100.2	118.1	N/A
3	99.9	101.3	90.7
4	100.4	104.3	N/A
5	100.1	94.0	90.9
6	100.1	93.3	89.9
7	100.0	95.8	95.3
8	100.2	98.7	94.3
9	100.2	91.1	91.7
10	100.0	95.0	95.7
11	100.0	97.9	97.5

Table 16. Data Related to the Product Extractions

I. Extraction #1
(2 ml aliquot, of 500 ml filtrate dilution)

Run #	Unextracted Sample Weight, (g)	Extracted Residue Weight, (g)	Aliquot Vial Label Code
3	10.88	6.96	N/A
3	10.57	6.54	#3-1
5	10.35	6.82	#5-1
5	10.86	7.02	N/A
6	10.28	6.99	#6-1
7	10.98	7.00	#7-1
8	10.38	6.99	#8-1
9	10.51	6.40	#9-1
10	10.82	5.75	#10-1

Note: Run #10 yielded 68 g of material suitable for extraction, or about 71 % of the reacted sample weight.

Table 16, continued

II. Extraction #2
(2 ml aliquot, of 500 ml filtrate dilution)

Run #	Unextracted Sample Weight, (g)	Extracted Residue Weight, (g)	Aliquot Vial Label Code
3	10.31	6.55	#3-2
5	10.87	7.26	#5-2
6	10.19	6.76	#6-2
7	10.71	7.45	#7-2
8	10.03	6.73	#8-2
9	11.24	6.99	#9-2
10	10.52	6.12	#10-2

Note: Run #10 yielded 68 g of material suitable for extraction, or about 71 % of the reacted sample weight.

III. Extraction #3
(10 ml aliquot, of 500 ml filtrate dilution)

Run #	Unextracted Sample Weight, (g)	Extracted Residue Weight, (g)	Aliquot Vial Label Code
3	3.17	1.19	#3-3
5	2.78	0.91	#5-3
6	2.68	1.06	#6-3
7	2.26	0.76	#7-3
8	2.71	0.92	#8-3
9	2.64	0.99	#9-3
10	2.87	0.97	#10-3

Note: Run #10 yielded 68 g of material suitable for extraction, or about 71 % of the reacted sample weight.

Table 17. Summary of Sugar Analysis by High-Performance Liquid Chromatography.

Sample #	Glucose Yield			Xylose Yield		
	mmol/g [a]	g/g [b]	% [c]	mmol/g [a]	g/g [b]	% [c]
3-2	0.609	0.110	16.1	0.225	0.034	14.6
3-3	1.015	0.183	26.8	0.366	0.055	23.7
5-2	0.484	0.087	12.8	0.156	0.023	10.1
5-3	0.908	0.163	24.0	0.319	0.048	20.7
6-2	0.598	0.108	15.6	0.152	0.023	9.7
6-3	1.356	0.244	35.4	0.397	0.060	25.5

Notes:

[a] mmol sugar/g HF-reacted solid (after N_2 and vacuum desorption)

[b] g sugar/g HF-reacted solid (after N_2 and vacuum desorption)

[c] % theoretical yield back-calculated to original wood given the weight of the HF-reacted solid (after N_2 and vacuum desorption) and the weight of the original wood charge.
Theoretical glucose yield: 3.441 mmol/g-wood
Theoretical xylose yield: 1.4 mmol/g-wood

[d] Samples with #-2 designation: portion of HF-reacted solid soluble in tepid water; posthydrolysis of water-soluble products in 2 N TFA at 121 °C for 1 hr, i.e. posthydrolysis of water-soluble products only.

[e] Samples with #-3 designation: the HF-reacted solid was autoclaved in 3% (wt.) sulfuric acid at 121 °C for 1 hr, i.e. posthydrolysis of entire HF-reacted solid.